

Structure-Based Design, Synthesis, and A-Site rRNA Cocrystal Complexes of Functionally Novel Aminoglycoside Antibiotics: C2'' Ether Analogues of Paromomycin

Stephen Hanessian,*[†] Janek Szychowski,[†] Susanta Sekhar Adhikari,[†] Guillermo Vasquez,[‡] Pachamuthu Kandasamy,[†] Eric E. Swayze,[‡] Michael T. Migawa,[‡] Ray Ranken,[‡] Boris François,[§] Julia Wirmer-Bartoschek,[§] Jiro Kondo,[§] and Eric Westhof[§]

Department of Chemistry, Université de Montréal, C. P. 6128, Succ. Centre-Ville, Montréal, P. Q., Canada, H3C 3J7, Isis Pharmaceuticals, 2292 Faraday Drive, Carlsbad, California 92008, and Institut de Biologie Moléculaire et Cellulaire UPR9002 CNRS, Université Louis Pasteur, 15 rue René Descartes, 67084 Strasbourg Cedex, France

Received October 14, 2006

A series of 2''-O-substituted ether analogues of paromomycin were prepared based on new site-selective functionalizations. X-ray cocrystal complexes of several such analogues revealed a new mode of binding in the A-site rRNA, whereby rings I and II adopted the familiar orientation and position previously observed with paromomycin, but rings III and IV were oriented differently. With few exceptions, all of the new analogues showed potent inhibitory activity equal or better than paromomycin against a sensitive strain of *S. aureus*. Single digit μM MIC values were obtained against *E. coli*, with some of the ether appendages containing polar or basic end groups. Two analogues showed excellent survival rate in a mouse septicemia protection assay. Preliminary histopathological analysis of the kidney showed no overt signs of toxicity, while controls with neomycin and kanamycin were toxic at lower doses.

Introduction

Aminoglycoside antibiotics have occupied a time-honored position in the hierarchy of antibacterial agents for over half a century.¹ Since the discovery of streptomycin in 1944,² several members of this class of polycationic pseudo-oligosaccharides have been used in clinical practice.³ Gentamicin, tobramycin, and amikacin are representatives of the more commonly used aminoglycosides, especially for Gram-negative infections. Although the aminoglycosides exhibit potent bactericidal activity, their widespread use has been compromised by dose-related nephrotoxicity and ototoxicity.⁴ For these and other reasons, aminoglycoside therapy is confined to a hospital environment, and i.v. administration requires careful monitoring. As with other antibiotic regimens, their use as the primary treatment of life-threatening infections has also been curtailed due to the rapid emergence of resistant strains of bacteria.^{3–5} This has instigated extensive research efforts on several fronts in search of new, or chemically modified, antibiotics that can delay or avoid acquired resistance by pathogenic bacteria.

Although a large number of antibiotic entities have been introduced in the market during the past two decades, very few if any new aminoglycosides have been reported, except for alternative formulations. For example, tobramycin is available as an effective treatment for the prevention of infection in cystic fibrosis patients as an inhaler formulation.⁶ The intrinsic potency of aminoglycosides makes them excellent candidates to explore new ways to overcome bacterial resistance and diminish toxicity. In this paper, we report our efforts in the design and synthesis of modified analogues of paromomycin and the discovery of a new paradigm toward the interaction of functionally diverse ether appendages at C2'' within the A-site subunit.

Paromomycin **1**, belongs to the 4,5-disubstituted class of 2-deoxystreptomine-containing aminoglycosides (Figure 1).

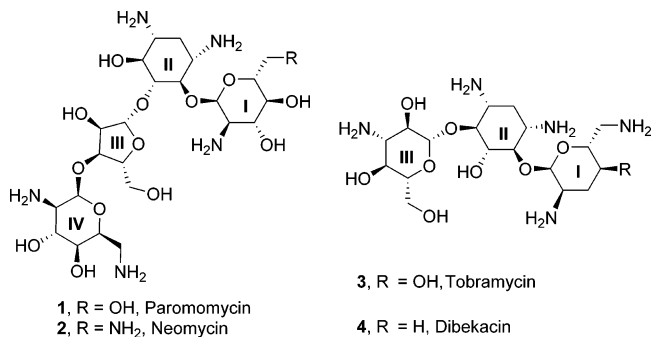


Figure 1. Structures and simulated bioactive conformations of paromomycin, tobramycin, and dibekacin.

Although its structure and stereochemistry has been known for many decades,⁷ its use in clinical practice has been limited due to its poor therapeutic index. Its closest analogue, neomycin **2**, is commonly used in ointment preparations for external use.⁸ Like all other aminoglycosides possessing a hydroxyl group at C3' of ring I, paromomycin is subject to phosphorylation by *O*-phosphoryltransferases, rendering it devoid of activity.^{5,9} Although deoxygenation at this site, as in tobramycin **3** and dibekacin **4**, prevents modification by these enzymes, other modes of enzymatic inactivation exist (*N*-acetyltransferases, *O*-adenyltransferases)^{3,5} that eventually diminish the efficacy of aminoglycosides as antibacterials. Added to these natural defense mechanisms by resistant bacteria are other hurdles to overcome such as reduced permeability,¹⁰ efflux pumps,¹¹ and target modification¹² within bacteria. Despite these major obstacles, potential solutions can be envisaged thanks to the important contributions in understanding the mode of antibacterial action of aminoglycosides.¹³ They inhibit protein biosynthesis by disrupting the fidelity of tRNA selection step involved in the binding process to the A-site of bacterial ribosome 16S RNA. Codon misreading in this highly conserved sequence of nucleotides affects translation and recognition of the mRNA sequence, leading to aberrant translation and interruption in protein synthesis.

* To whom correspondence should be addressed. Phone: 514-343-6738. Fax: 514-343-5728. E-mail: stephen.hanessian@umontreal.ca.

[†] Université de Montréal.

[‡] Isis Pharmaceuticals.

[§] Université Louis Pasteur.

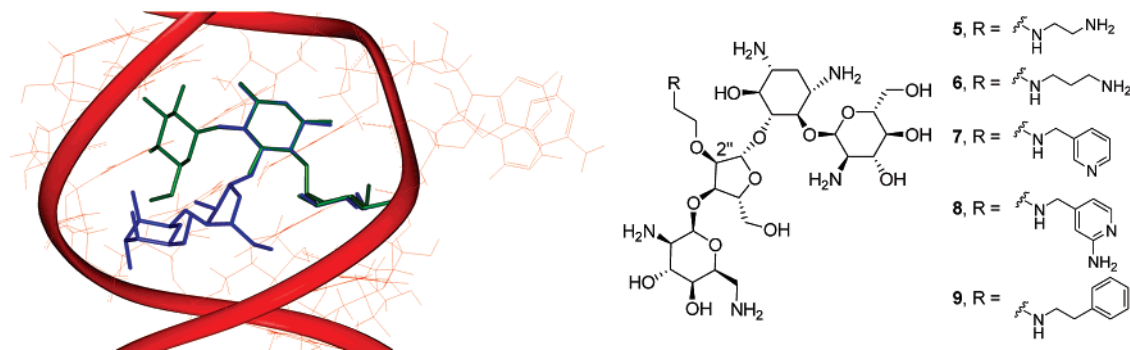


Figure 2. Paromomycin C2'' ethers complexed for X-ray study. Left: superposition of paromomycin (blue) with tobramycin (green) from their respective X-ray complexes; Right: structures of active C2'' ethers (**6–8**) cocrystallized with A-site oligonucleotides.

The relevance of these elegant biochemical studies was rendered all the more important with seminal contributions toward the elucidation of the molecular structure of the ribosome,¹⁴ especially the high-resolution crystal structures of bacterial ribosomal 30S particles complexed to aminoglycosides.¹⁵ The crystal structures of aminoglycoside complexes with the decoding A-site of the bacterial ribosome 16S RNA have been solved with excellent resolution (2.4–2.54 Å).¹⁶ Studies of aminoglycoside–RNA complexes have also been reported by biochemical,¹⁷ spectroscopic,¹⁸ mass spectrometric,¹⁹ and NMR techniques.²⁰ Recent insights into molecular modeling have provided further tools to probe such interactions *in silico*.²¹

Paromomycin in particular, exhibits strong binding to the A-site of 16S RNA by making effective contacts through amino and hydroxyl groups while adopting a unique bioactive L-shaped conformation, as seen in the crystal structure of the complex.^{16a} Thus, ring I is inserted into the A-site helix by forming a pseudo base pair with two H-bonds to the Watson–Crick sites of A1408 and benefiting from a stacking interaction against G1491. In the process, the A1492 and A1493 residues are sequestered in the bulged out conformation, allowing them to make Watson–Crick interactions with two base pairs in the minor groove. This hallmark event of maintaining an “out” conformation for A1492 and A1493 in the aminoglycoside docked complex, forms the molecular basis for codon misreading. The deoxystreptamine (ring II) unit also makes contacts with different nucleotides, which in conjunction with ring I, contributes to recognition, binding, and stabilization. Rings III and IV, forming the lower arm of the L-shaped structure, contribute to binding affinity and charge interactions of phosphates, as well as correctly orienting rings I and II in the bioactive conformation.

These enormously informative insights into the molecular basis of aminoglycoside interactions at the ribosomal level have instigated renewed interest in the field.²² The charged anionic nature of the rRNA subunits responsible for recognition led to the logical derivatization of aminoglycosides with a variety of pendant basic side chains. Indeed, in many cases, interesting *in vitro* antibacterial activities were reported.^{22f} With one exception,²³ there are no X-ray structural data to delineate possible beneficial interactions of such multidentate aminoalkyl appendages with the A-sites subunit.

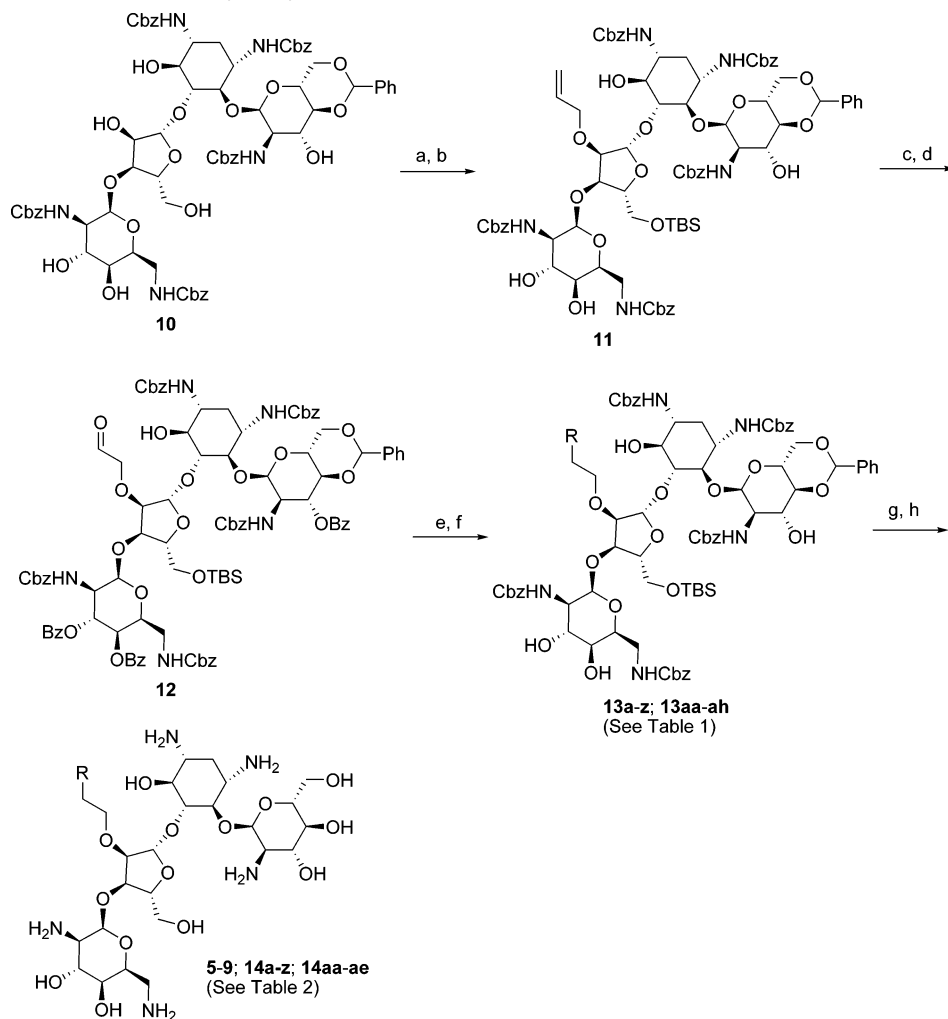
Our strategy toward the design of new aminoglycoside analogues was to take advantage of the structural information available from X-ray complexes and to exploit the reactivity pattern of paromomycin toward new sites for derivatization to install functionality capable of making productive contacts. Herein, we report the results of such efforts.

Design

Westhof and co-workers²⁴ have shown that rings I and II of paromomycin **1** and tobramycin **3** occupy the same site, and they are virtually superimposable in their respective X-ray cocrystal structures in the RNA A-site (Figure 2). Inspection of the perspective diagrams led us to the realization that the introduction of aminoalkyl ethers at C2'' (or C6) hydroxyl groups, hitherto unexplored sites in the paromomycin framework, might lead to analogues with a hybrid function. Preliminary modeling showed that *a priori*, such C2'' ethers containing a basic group derived from paromomycin could reach the space occupied by ring III of tobramycin and possibly simulate one of its amino groups. We were pleased to find that the C2'' (2-aminoethyl-amino) ethyl and the C2'' (3-aminopropyl-amino) ethyl ether derivatives **5** and **6** of paromomycin (Figure 2) showed *in vitro* activity against *S. aureus* comparable to that of the parent antibiotic (see SAR below). However, the activity was an order of magnitude less than that of tobramycin. Although several other acyclic ethers were also prepared (see below), we shifted the logic-based paradigm of aliphatic *N*-aminoalkyl ether appendages at C2'' to include *N*-aryllalkyl and *N*-heteroarylalkyl counterparts (compounds **7–9**, for example). This radical design concept led to the synthesis of a series of highly active C2'' ether tethered analogues (see SAR below).

Chemistry

The readily available paromomycin derivative **10**²⁶ was transformed first to the corresponding 5''-OTBS ether and then *O*-allylated at C2'' in the presence of allyl iodide and KHMDS to give **11** in good overall yield (Scheme 1). The selective *O*-alkylation at C2'' was ascertained by methanolysis with TMSCl in MeOH and MS analysis of the resulting paromamine and *O*-allylated methyl paromobiosaminide subunits. Benzoylation followed by ozonolysis led to the selectively protected benzoate ester **12**. It should be noted that the *O*-benzoylation of **11**, containing four secondary hydroxyl groups, afforded a product in which the C6 hydroxyl group remained free, presumably due to steric reasons. A series of reductive aminations led to the respective aminoethyl ethers **13a–z** and **13aa–ah** (See Table 1). Cleavage of the benzoate esters in the presence of MeONa in MeOH, followed by treatment with aqueous acetic acid and hydrogenolysis, gave the corresponding C2'' *O*-substituted paromomycin analogues **5–9**, **14a–z**, and **14aa–ae** as their peracetate salts. The *N*-acetyl and *N*-benzoyl derivatives **9a** and **9b** were also prepared from **13e** (not shown, see Table 2). To assess the importance of ring IV in the ether analogues, we devised a mild method of oxidative cleavage of

Scheme 1. C2'' Modification of Paromomycin by Reductive Amination^a

^a Reagents and conditions: (a) TBSOTf, 2,4,6-collidine, CH₂Cl₂, 75%; (b) CH₂=CHCH₂I, KHMDS, THF, 70%; (c) BzCl, pyridine, DMAP, 95%; (d) (i) O₃, CH₂Cl₂, -78 °C; (ii) Me₂S, -78 °C to RT, 80%; (e) amine, NaBH₃CN, MeOH/AcOH (30:1), 90%; (f) MeONa/MeOH; (g) AcOH/H₂O (4:1), 60 °C, 2 h; (h) Pd(OH)₂/C, H₂, AcOH/H₂O (4:1).

the vicinal diol, followed by base-catalyzed elimination, to give representative ring I, II, and III pseudotrisaccharides²⁶ (Scheme 2). Thus, treatment of **11** with Pb(OAc)₄ in pyridine resulted in the cleavage of the 3''',4'''-diol to give a dialdehyde, which underwent β-elimination upon treatment with Et₃N to give **15**. Conversion to the benzoate **16** and ozonolysis of the allyl ether followed by reductive amination and debenzoylation gave the products **17a–c**. Final deprotection of the acetal as well as the OTBS ether and hydrogenolysis of the N-Cbz groups gave the intended ring IV truncated analogues **18a–c**.

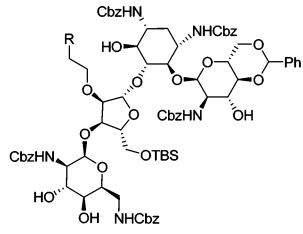
We next addressed the synthesis of neutral alkyl ethers at C2'' of paromomycin (Scheme 3). TBS protection of the primary alcohol followed by alkylation of **10** with cinnamyl bromide in the presence of KHMDS and Bu₄NI at 0 °C gave **19** in 70% yield. Alternatively, the same product could also be obtained by performing a cross-metathesis reaction of **11** with styrene in the presence of the Grubbs second generation catalyst²⁷ in 75% yield. Cleavage of the benzylidene acetal as well as the OTBS ether followed by catalytic hydrogenolysis gave **20**. Extended and truncated *N*-aryl ether analogues of paromomycin were also prepared (Scheme 4). Thus, a Wittig reaction of **12** gave **21** as a mixture of isomeric olefins. Deprotection and hydrogenation afforded the 5-phenylpentyl ether analogue **22**. Treatment of **12** with phenylmagnesium bromide or diphenyl zinc gave **23** as a mixture of two alcohols. Acidic cleavage of

the acetal and TBS groups, followed by hydrogenolysis, gave **24** or **25**, depending on the length of the reaction time.

Finally, we also deemed it necessary to prepare a 3-phenylpropyloxy ether to complete this series in which nitrogen, carbon, or oxygen atoms were part of the ether chain (Scheme 5). Thus, reduction of **12** led to the alcohol **26**, which was deprotected to give **27**. The alcohol **26** was also transformed into **28** by standard alkylation with cinnamyl bromide and afforded **29** upon global deprotection.

X-ray Structures of Complexes between the Aminoglycosides and A-Site RNA. The overall conformations of the A-site complexed with **6**, **7**, and **8** are almost the same as those of the previous RNA/aminoglycoside complexes.^{16,25} (Figure 3a–c). At both ends of the internal loop of the A-site, canonical Watson–Crick pairs, G1405 = C1496, G1494 = C1407, and C1409 = G1491 are formed (Figure 3d,f,h). The U1406 residue forms a bifurcated base pair with the U1495 residue (Figure 3e). The A1408 residue, which is conserved in bacteria, does not form any base pair (Figure 3 g). All complexes between oligonucleotides containing the A-site and paromomycin derivatized at the 2'' position present the same structural characteristics as previously published.²⁵ A cocrystal structure of **6** with the A-site oligonucleotides presented the same structural characteristics seen in paromomycin complex.^{16a} (Figure 3a).

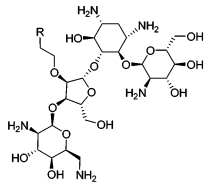
Table 1. Side Chains in Compounds 13a–z and 13aa–ah



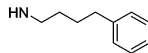
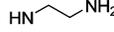
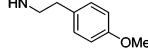
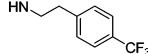
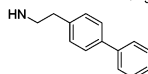
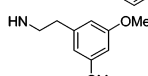
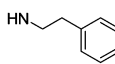
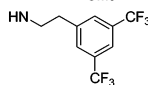
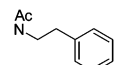
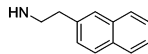
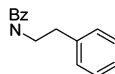
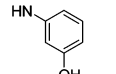
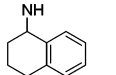
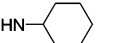
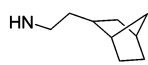
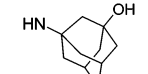
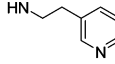
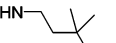
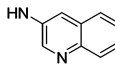
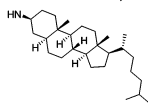
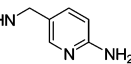
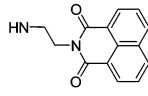
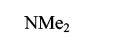
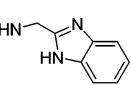
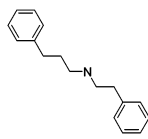
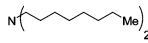
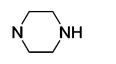
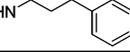
Compound	R	Compound	R	Compound	R
13a		13m		13y	
13b		13n		13z	
13c		13o		13aa	
13d		13p		13ab	
13e		13q		13ac	
13f		13r		13ad	
13g		13s		13ae	
13h		13t		13af	
13i		13u		13ag	
13j		13v		13ah	
13k		13w			
13l		13x			

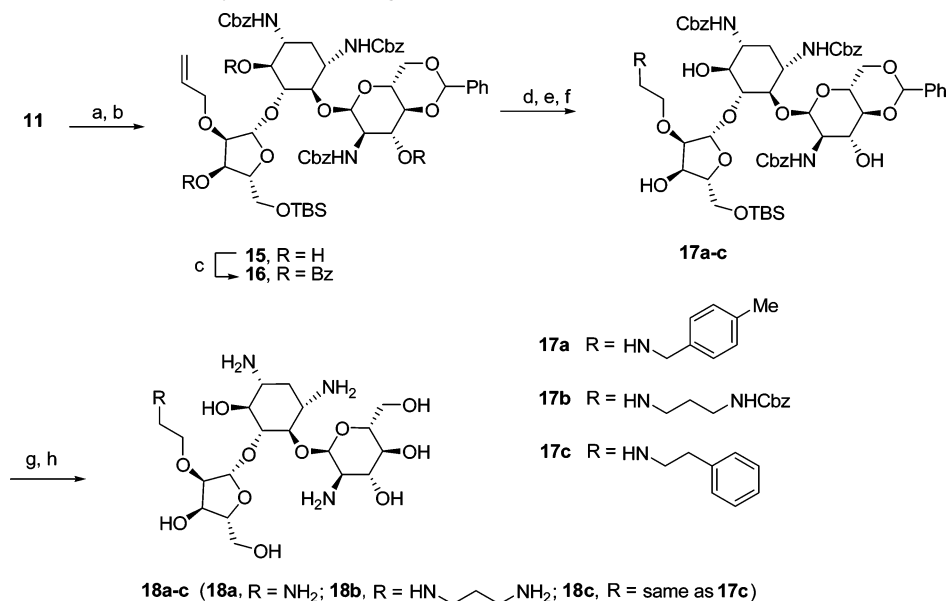
The paromamine moiety makes contact with the three conserved adenines (A1408, A1492, and A1493). On the other hand, the conformation of ring III is changed, and the rotation about the linkage between rings II and III leads to a global rotation of ring IV by 90°. The hydroxyl group O5'' has rotated by 90° and forms two H-bonds with the Hoogsteen sites of G1491. Intrigued by the potent inhibitory activity of compounds **7** and **8**, we obtained X-ray structures of their complexes (Figure 3b,c). As previously observed,²⁵ the β-D-ribofuranosyl ring was turned by 40° with respect to the paromamine unit, which, together with a change in the sugar pucker (C3'' endo instead of C2'' endo), results in a 90° change in the orientation of ring IV in the new analogue **8**. While the oxygen atom in the ring III still forms an intermolecular H-bond with C2'NH₂ of ring I, the

hydroxymethyl group at C5'' forms an H-bond with O6 of G1491 instead of N7, as in the case of paromomycin. A network of additional H-bonds can be observed resulting in new interactions. The new ether chain at C2'' extends across the deep major groove of the A-site and points into the solvent (Figure 3i). These unprecedented conformational changes and new interactions as a result of the incorporation of a C2'' ether chain result in a compactly folded paromomycin structure with unique binding sites. In the case of compound **8**, the primary amine of the aromatic ring forms two H-bonds with anionic phosphate oxygen atoms (O2P of G1491 and O1P of U1490). In addition, two water molecules bridge the N7'' with the O2P of G1405. Compound **8** makes 15 direct contacts with the A-site nucleotides and three indirect contacts mediated by water molecules

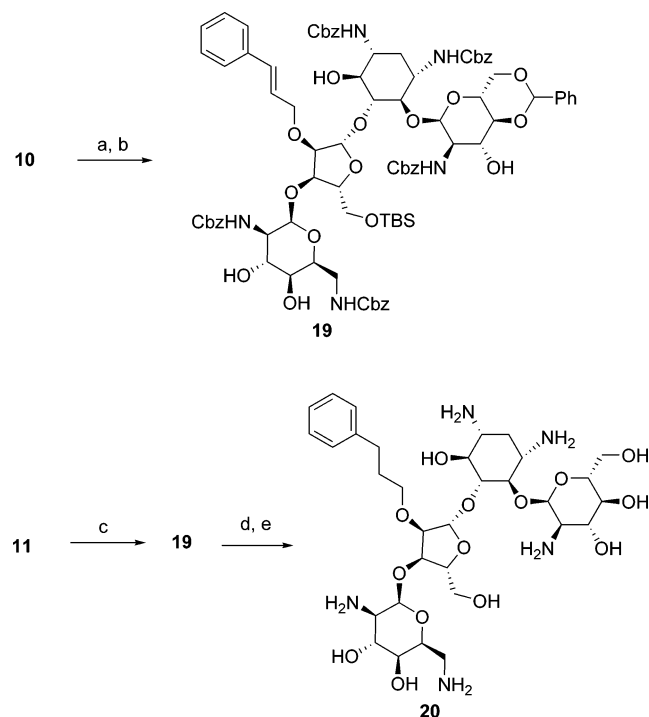
Table 2. Activities of Paromomycin C2'' Ether Analogues


The image shows the chemical structure of Paromomycin C2'' Ether Analogue, a complex polyamine molecule with multiple hydroxyl and amino groups, and a variable R group attached to the C2'' position.

Compound	R	MIC		Compound	R	MIC	
		$\mu\text{g/mL}$ <i>E. coli</i>	$\mu\text{g/mL}$ <i>S. aureus</i>			$\mu\text{g/mL}$ <i>E. coli</i>	$\mu\text{g/mL}$ <i>S. aureus</i>
1	-	3-6	1-2	14m		10-20	3-5
5		6-12	2-3	14n		5-10	<0.6
6		25-50	3-6	14o		5-10	0.6-1.2
7		12-25	<1.5	14p		20-40	5-10
8		6-12	0.6-1	14q		10-20	5-10
9		3-6	0.3-0.6	14r		>10	2.5-5
9a		10-20	1-3	14s		10-20	1-3
9b		10-20	1-3	14t		12-25	2-3
14a		12-25	2-3	14u		>10	1.25-2.5
14b		1.5-3	3-6	14v		3-6	3-5
14c		1.5-3	3-6	14w		>10	5-10
14d		12-25	<1.5	14x		20-40	1-3
14e		12-25	<1.5	14y		10-20	0.6-1
14f		12-25	1-2	14z		>10	2.5-5
14g		3-6	0.3-0.6	14aa		>40	10-20
14h		12-25	2-3	14ab		12-50	6-12
14i		>100	>100	14ac		10-20	0.6-1.2
14j		50-100	6-12	14ad		5-10	1.2-2.5
14k		3-6	3-5	14ae		25-50	2-3
14l		3-5	0.6-1.2				

Scheme 2. C2'' Modification of Paromomycin without Ring IV^a

^a Reagents and conditions: (a) Pb(OAc)₄, pyridine; (b) Et₃N, THF, 30%, two steps; (c) BzCl, pyridine, DMAP, 95%; (d) (i) O₃, CH₂Cl₂, -78 °C; (ii) Me₂S, -78 °C to RT, 80%; (e) amine, NaBH₃CN, MeOH/AcOH (30:1), 90%; (f) MeONa/MeOH; (g) AcOH/H₂O (4:1), 60 °C, 2 h; (h) Pd(OH)₂/C, H₂, AcOH/H₂O (4:1).

Scheme 3. C2'' Modification of Paromomycin with a Carbon Side Chain^a

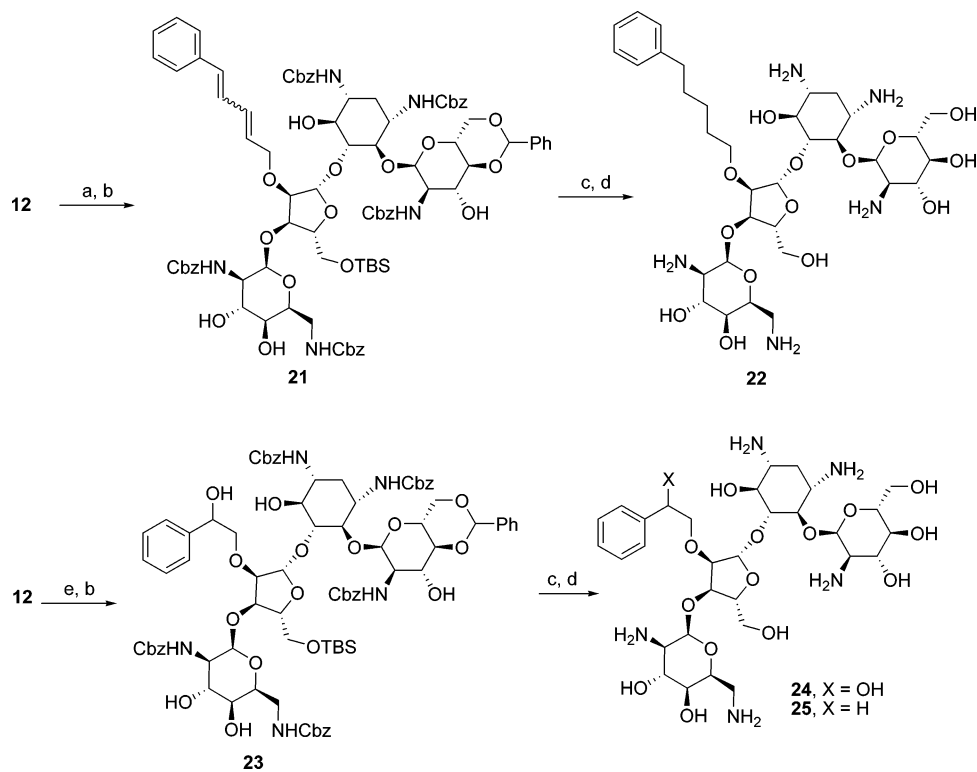
^a Reagents and conditions: (a) TBSOTf, 2,4,6-collidine, CH₂Cl₂, 75%; (b) cinnamyl bromide, KHMDS, Bu₄NI, THF, 70%; (c) Grubbs II, styrene, CH₂Cl₂, reflux, 16 h, 75%; (d) AcOH/H₂O (4:1), 60 °C, 2 h; (e) Pd(OH)₂/C, H₂, AcOH/H₂O (4:1), 70% for two steps.

(see Figure 3d–h), while paromomycin forms 12 direct contacts. Compound **8** also has the lowest dissociation constant from the 16S RNA and the best MICs. By contrast, compounds **6** and **7** form, respectively, 11 and 12 direct contacts, while paromomycin forms 12 direct contacts. Thus, the expected extension of C2''-aminoalkyl ether appendages toward ring III of tobramycin was not realized. Instead, a new mode of binding of these

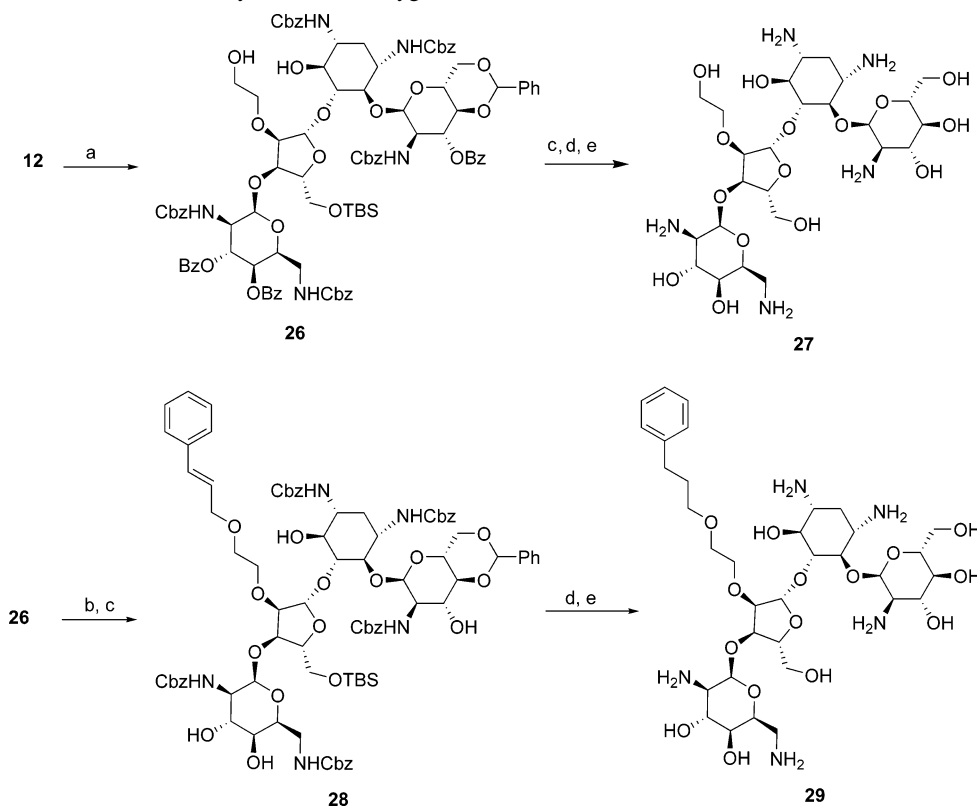
paromomycin derivatives was discovered leading to potent in vitro and in vivo (mouse) activity.

Biological Results and Discussion

All compounds were tested for activity against *E. coli* (ATCC#25922) and *S. aureus* (ATCC#13709). The minimum inhibitory concentrations are shown in Tables 2–4. As shown in Table 2, the SAR series of 2''-ethylamino-substituted paromomycin analogues encompasses a variety of lipophilic and lipophobic functionality, as well as aliphatic and aromatic moieties. The steric space around the C2''-position has been explored using relatively small and large bulky substituents at the extremity of the side chain. With few exceptions, all of these modifications at the C2''-position were well tolerated against *S. aureus* (ATCC#13709), while the smaller, aliphatic, and polar functionalities seemed to fare better against *E. coli* (ATCC#25922). In the *E. coli* series, this is further confirmed by the reduced activity of the nonpolar carbon and oxygen analogues shown in Table 4, which is consistent with the presence of a relatively large pocket about the C2'' side chain in the A-site, which is unoccupied. Substitution at C2'' orients the III–IV rings in the A-site in a manner different from that of unsubstituted paromomycin and places the side-chain substituents in the deep major groove of the A-site. In fact, even quite large and bulky substituents (for example, **14w**, **14x**, **14z**, **14aa**, **14ac**, and **14ad**) displayed activity close to, or better than, that of paromomycin against *S. aureus*. This fact allows one to append functionality that could drastically alter the pharmacokinetic properties of the aminoglycosides, potentially avoiding enzymes that confer resistance and possibly alter the toxicity profile. While these factors have yet to be ascertained, we had surmised that the alternative mode of binding for the C2''-substituted analogues in paromomycin places ring IV in an orientation that does not benefit from critical interactions within the A-site. As can be seen in Table 3, removal of ring IV of the C2''-substituted analogues results in active compounds, while the paromomycin analogue is totally inactive. Although the activity of C2'' ethers lacking ring IV is slightly reduced compared to that of the parent analogue, the loss of ring IV is

Scheme 4. C2'' Modification of Paromomycin with a Carbon Side Chain^a

^a Reagents and conditions: (a) cinnamyl triphenylphosphonium bromide, KHMDs, THF, 60%; (b) MeONa/MeOH, 80%; (c) AcOH/H₂O (4:1), 60 °C, 2 h; (d) Pd(OH)₂/C, H₂, AcOH/H₂O (4:1), 70% for two steps; (e) Ph₂Zn, RT, 90% or PhMgBr, -40 °C, 70%.

Scheme 5. C2'' Modification of Paromomycin with an Oxygen Side Chain^a

^a Reagents and conditions: (a) NaBH₃CN, MeOH/AcOH (30:1), 80%; (b) cinnamyl bromide, KHMDs, THF, Bu₄NI, 45%; (c) MeONa/MeOH, 80%; (d) AcOH:H₂O (4:1), 60 °C, 2 h; (e) Pd(OH)₂/C, H₂, AcOH/H₂O (4:1), 70% for two steps.

not as detrimental. Thus, ring IV appears to be less important for binding in the C2'' ether series.

To determine whether our analogues would have in vivo activity, compounds **7** and **9** were chosen to test in a mouse

septicemia protection assay. Mice were infected IP with *S. aureus* and treated at 1 h and 3 h post-infection with drug delivered subcutaneously. All nondrug-treated mice were moribund within 12 h and were sacrificed within 18 h. As shown in

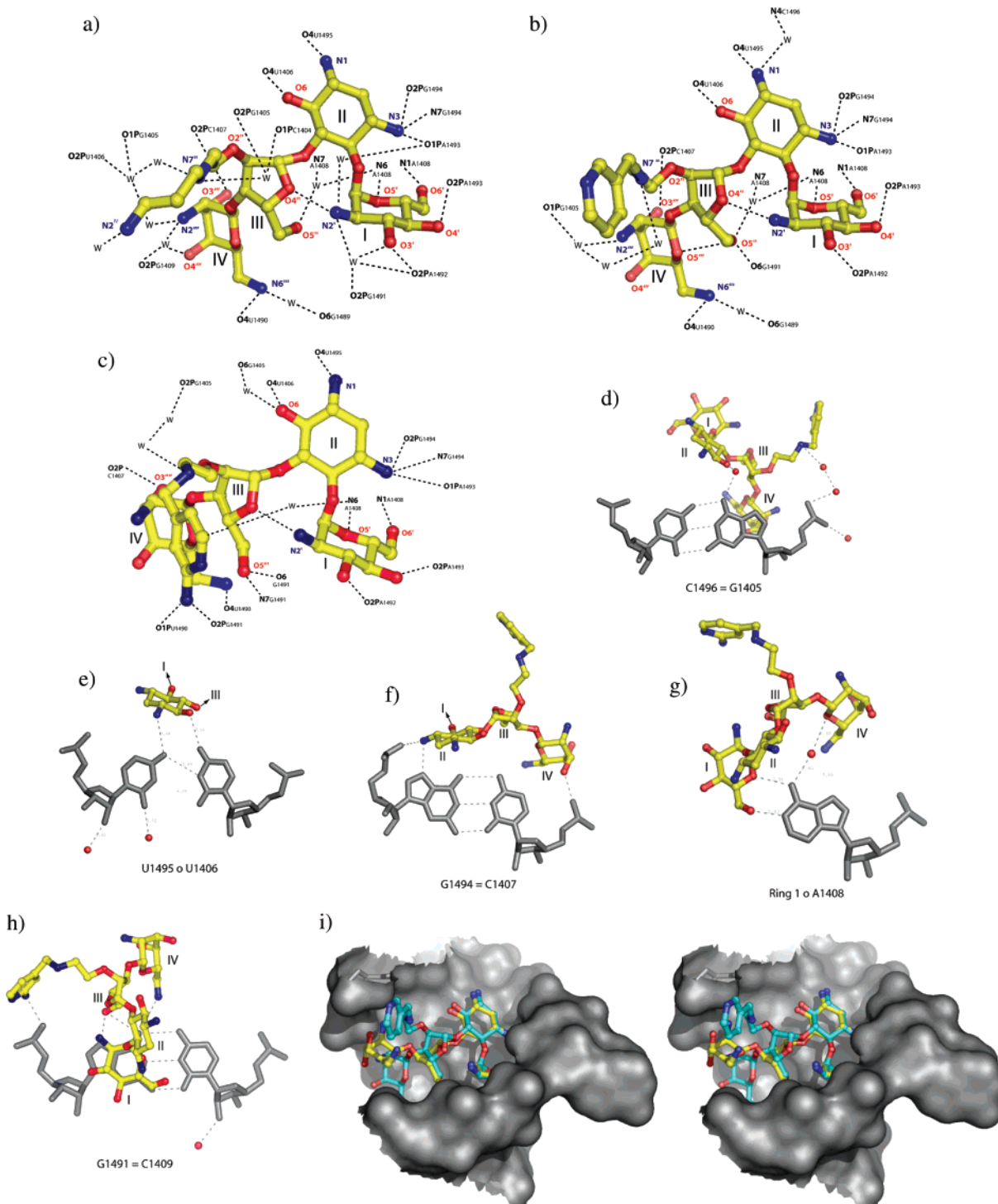
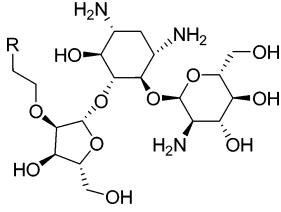


Figure 3. X-ray complexes of analogues **6–8** with the A-site. (a), (b), and (c): Molecular contacts of **6**, **7**, and **8**, respectively, with A-site RNA. The structures for **6** and **7** were previously published.²⁵ Hydrogen bonds are represented by dashed lines and water molecules are represented by the letter w. (d), (e), (f), (g), and (h): Interactions between **8** and the base present in the A-site. Water molecules are represented by red spheres. (i): Stereoview of **7** (green) superimposed with paromomycin **1** (yellow).

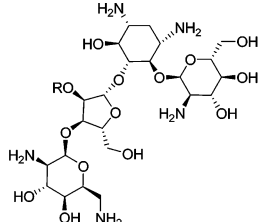
Table 5, compound **7** fully protected mice at 1.2 mg/kg. Compound **9** showed an ED₉₀ at 0.25 mg/kg and fully protected the mice at 0.50 mg/kg. Furthermore, compound **7** showed no overt signs of toxicity after observation of the mice up to two weeks and after performing a histopathological analysis of the kidney (data not shown). Compound **9** did display some acute toxicity at the highest dose (75 mg/kg × 2), indicating the phenethyl analogue was slightly more toxic. It is interesting to note that histopathological analysis of the control aminoglycosides indicated kidney toxicity at a lower dose (37 mg/kg × 2).

Clearly, these preliminary promising tests warrant further validation in more extensive animal studies.

The useful information that we have obtained from our X-ray data has guided our SAR in several significant ways. While it should be noted that the improvement in activity in animal models correlates well with the improvement in MIC activity, this is most likely due to more favorable pharmacokinetic properties. However, these improvements, due to extension of the C-2'' side chain, are greatly aided by the structural information we have obtained. In particular, the extent of

Table 3. Activities of Paromomycin C2'' Ether Analogues without Ring IV


compound	R	MIC ($\mu\text{g/mL}$) <i>E. coli</i>	MIC ($\mu\text{g/mL}$) <i>S. aureus</i>
1	—	3–6	1–2
1 without ring IV	—	>100	>100
18a	NH ₂	6–12	12–25
18b	HN—CH ₂ —CH ₂ —CH ₂ —NH ₂	6–12	6–12
18c	HN—CH ₂ —C ₆ H ₅	>100	12–25

Table 4. Activities of Paromomycin C2'' Ether Analogues with Carbon or Oxygen Side Chains


Compound	R	MIC ($\mu\text{g/mL}$) <i>E. coli</i>	MIC ($\mu\text{g/mL}$) <i>S. aureus</i>
1	—	3–6	1–2
20	H ₂ C—CH ₂ —C ₆ H ₅	20–40	3–5
22	H ₂ C—(CH ₂) ₄ —C ₆ H ₅	10–20	3–5
24	H ₂ C—CH(OH)—C ₆ H ₅	25–50	3–6
25	H ₂ C—C ₆ H ₅	>50	6–12
27	OH	12–25	12–25
29	H ₂ C—O—(CH ₂) ₄ —C ₆ H ₅	20–40	5–10

Table 5. Compounds **7** and **9** in a Mouse Septicemia Protection Assay^a

cmpd	number of mice moribund/total number of mice (dosage (mg/Kg))									
	(0.13)	(0.25)	(0.50)	(1.2)	(2.3)	(4.7)	(9.4)	(19)	(38)	(75)
7	7/10	6/10	3/10	0/10	0/10	0/10	0/10	0/10	0/10	0/10
9	5/10	1/10	0/10	0/10	0/10	0/10	0/10	0/10	0/10	4/10

^a Compounds were dosed at the indicated amounts at 1 h and 3 h post *S. aureus* infection.

toleration of the C-2'' side chain is quite impressive due to the alternative mode of binding and suggests further points of contact could be made in this pocket. Our X-ray studies have shown that new contacts are possible within the A-site. Furthermore, this new mode of binding predicts a reduced

importance of the ring IV when a C-2'' substituent is present. This is also borne out experimentally in the SAR.

Conclusion

The remarkable potency of the C2''-substituted ether analogues and their apparent reduced toxicity, exemplified by analogue **7**, demonstrate the potential of this series in addressing the issues observed with aminoglycosides in a clinical setting. Moreover, the alternative mode of binding adopted by the C2''-substituted analogues allows a high tolerance for substitution at the C2''-position and for additional modification, including removal of ring IV. Additional work to ascertain their susceptibility to resistance conferring enzymes, efflux pumps, and broader antibacterial activities are underway. The encouraging mouse protection results augur well for more extensive in vivo studies with different bacterial strains of clinical relevance.

Experimental Section

In Vitro Studies. Minimum Inhibitory Concentrations (MICs, Bacteria). The assays are carried out in 150 μL volume in duplicate in 96-well, clear, flat-bottom plates. The bacterial suspension from an overnight culture growth in appropriate medium is added to a solution of test compound in 2.5% DMSO in water. Final bacterial inoculum is approximately 10^2 – 10^3 CFU/well. The percentage growth of the bacteria in test wells relative to that observed for a control well containing no compound is determined by measuring absorbance at 595 nm (A_{595}) after 20–24 h at 37 °C. The MIC is determined as a range of concentrations, where complete inhibition of growth is observed at the higher concentration and bacterial cells are viable at the lower concentration. Both ampicillin and tetracycline are used as antibiotic positive controls in each screening assay for *E. coli* (ATCC#25922) and *S. aureus* (ATCC#13709).

In Vivo Studies. Bacteria. *Staphylococcus aureus* was obtained from American Type Culture Collection repository (Smith strain ATCC#13079). The bacterium was passaged several times through mice to achieve and maintain mouse virulence. To be virulent in mice, the *Staphylococcus aureus* needed to be suspended in 10% sterile hog gastric mucin (obtained from Sigma).

Mice. Female Balb/c mice (16–18 g) were obtained from Charles River Labs. The mice were allowed to acclimate for one week prior to use. The mice, when challenged with bacteria, showed symptoms within 12 h of infection and were moribund and subsequently sacrificed by 18 h. All treated groups had 10 mice per group.

Compounds Tested and Controls. Amikacin, tobramycin, and neomycin obtained from the U.S. Pharmacopia were used as positive control drugs. They were reconstituted in water and were used at concentrations of 37.5, 18.8, 9.4, 4.7, and 2.3 mg/kg. The control compounds protected the mice at all concentrations tested. Compounds **7** and **9** were dissolved in water and used at 75, 37.5, 18.8, 9.4, 4.7, 2.3, 1.17, 0.5, 0.25, and 0.125 mg/kg. The data are shown in Table 5.

Mouse Septicemia Protection Assay. Mice were infected IP (intraperitoneally) with 0.5 mL of 10^6 Staph. organisms suspended in 10% mucin. Mice were treated at 1 h and 3 h post-infection with either serially 2-fold diluted control drug or serially 2-fold dilutions of drug delivered in the amount of 0.5 mL subcutaneously. Group I was a titration of *S. aureus* from 10^9 through 10^6 to illustrate virulence. Group II was the mucin only control and illustrates the need for Staph./mucin suspension to produce virulence in the mouse. Group III was the Amikacin-treated control group. Group IV was the tubercidin-treated control group. Group V was the neomycin-treated control group. Group VI comprised compound **7** and group VII was the compound **9**-treated group. Mice were observed over a two week period.

Crystallizations, X-ray Experiments, and Structure Refinements. Crystallization procedures are essentially the same as published previously.^{16,25} The asymmetrical loop of the bacterial A-site was inserted between Watson–Crick pairs in sequences designed to fold as a double helix (See Figure S1 in Supporting

Information). Prior to crystallization, each paromomycin derivative was dissolved at 4 mM in 50 mM sodium cacodylate buffer (pH 6.4), and 2 mM RNA solution containing 100 mM sodium cacodylate (pH 6.4), 25 mM sodium chloride, and 5 mM magnesium sulfate was annealed by heating at 85 °C for 2 min, followed by slow cooling to 37 °C. Same volumes of RNA solution and aminoglycoside solution were mixed at 37 °C, and then the mixture was cooled slowly to room temperature (21–25 °C). Crystallizations were performed by the hanging-drop vapor diffusion method at 37 °C in conditions containing 1–6% 2-methyl-2,4-pentanediol, 1–5% glycerol, and 50 mM sodium cacodylate. X-ray experiments were performed using synchrotron radiation at beamline ID14-4 of the European Synchrotron Radiation Facility (ESRF; Grenoble, France). Images were processed with the HKL2000²⁸ and Crystalclear (Rigaku/MSC). The statistics of data collection and the crystal data are summarized in Table S1 (See Supporting Information). Initial phases were derived with the molecular replacement program AMoRe²⁹ using the coordinates of the crystal structure of the RNA/paromomycin complex (PDB code: 1J7T).^{16a} The atomic parameters of the structure were refined with the program CNS.³⁰ The parameters and topology files for the antibiotic molecules were obtained on the Hetero-compound Information Center-Uppsala server (University of Uppsala, Sweden).³¹ The statistics of structure refinement are summarized in Table S1 (See Supporting Information). All figures were drawn using The PyMOL Molecular Graphics system (2002), DeLano Scientific, San Carlos, CA (<http://www.pymol.org>).

Chemistry. General. Solvents were distilled under positive pressure of dry argon before use and dried by standard methods: THF from Na/benzophenone and CH₂Cl₂ from CaCl₂. All commercially available reagents were used without further purification. All reactions were performed under nitrogen atmosphere. NMR (¹H, ¹³C) spectra were recorded on AMX-300, ARX-400, and AV-400 spectrometers. Low- and high-resolution mass spectra were recorded using electrospray technique. Optical rotations were recorded in a 1 dm cell at ambient temperature. Analytical thin-layer chromatography was performed on precoated silica gel plates. Visualization was performed by ultraviolet light and/or by staining with ceric ammonium molybdate. Flash column chromatography was performed using (40–60 μm) silica gel at increased pressure.

4',6'-O-Benzylidene-penta-N-benzyloxycarbonyl paromomycin (10). Sodium carbonate (55.0 g, 0.523 mol) and CbzCl (20.00 mL, 0.139 mol) were added to paromomycin sulfate (30.00 g, 0.0271 mol) in water (500 mL). After 18 h under vigorous stirring, the water was decanted and the white precipitate was washed with water twice. A solution of triethylamine (97.00 mL, 0.697 mol) in methanol (600 mL) was added, followed by CbzCl (25.00 mL, 0.174 mol). After 5 h, the solvents were evaporated. The resulting penta-NCbz-paromomycin was purified by flash column chromatography over silica gel (5% MeOH/CH₂Cl₂). The obtained white solid was codistilled with pyridine (200 mL) three times and at half of the volume of the third codistillation, toluene (200 mL) was added, and the solvents were evaporated to dryness. Another codistillation with toluene (300 mL) was done before heating the flask at 60 °C under 10 mmHg vacuum for 12 h. Freshly distilled benzaldehyde (400 mL) was added to the resulting white solid, and sonication was done to bring it in solution. To the stirred mixture was added 4 Å molecular sieves (15 g) and formic acid (50.00 mL, 0.530 mol). After stirring for 12 h at room temperature, the mixture was slowly added to a stirred ice-cold solution of saturated aqueous NaHCO₃, extracted with ethyl acetate (3 times), and the organic layer was washed with water and dried over Na₂SO₄. The solvent was evaporated to dryness to afford a crude solid, which was purified by flash column chromatography over silica gel (3% MeOH/CH₂Cl₂) to obtain the known compound **10** (18.91 g, 63%).²⁶

4',6'-O-Benzylidene-2''-O-allyl-5''-O-*t*-butyldimethylsilyl-penta-N-benzyloxycarbonyl paromomycin (11). Compound **10** (6.00 g, 4.367 mmol), dried by two codistillations with toluene, was dissolved in CH₂Cl₂ (400 mL) and 2,4,6-collidine (1.15 mL, 8.735 mmol), followed by TBDMSOTf (0.50 mL, 2.184 mmol) added at 0 °C. After 18 h, 0.6 equiv of TBDMSOTf was added, and 6 h

later, some of the CH₂Cl₂ was evaporated to a smaller volume for washing with 0.5 M HCl twice and NaHCO₃. Drying with Na₂SO₄ and purification by silica gel chromatography (2% MeOH/CH₂Cl₂) gave the O5''-TBS monoprotected compound (4.86 g, 75%); *R*_f 0.6 (CHCl₃/EtOAc/MeOH (20:5:3)); ¹H NMR (300 MHz, CDCl₃) δ 7.60–7.10 (m, 30H), 5.60–3.00 (m, 41H), 2.20 (m, 1H), 1.30 (m, 1H), 0.83 (s, 9H), 0.01 (s, 6H); ESI-MS *m/z* calcd for C₇₆H₉₃N₅O₂₄Si [M + H]⁺, 1487.60580; found, 1488.9; TOF-HRMS found, 1488.60258. This O5''-protected compound (2.10 g, 1.411 mmol) was codistilled with toluene twice, and the residue was dissolved in dry THF (70 mL) in a flask covered with aluminum foil. Allyl iodide (1.29 mL, 14.11 mmol) was added followed by the dropwise addition of 0.5 M KHMDS solution in toluene (1.41 mL, 0.706 mmol). The mixture was stirred overnight at room temperature, then 0.3 equiv of KHMDS was added, and 6 h later, the reaction mixture was quenched with an aqueous solution of satd. NH₄Cl (2 mL) and water. THF was evaporated, the aqueous layer was extracted with ethyl acetate (3 times), and the organic layer was washed with a sodium thiosulfate solution and brine and dried over Na₂SO₄. The solvent was evaporated to dryness to afford a crude solid, which was purified by silica gel flash chromatography (1.5% MeOH/CH₂Cl₂), providing the known allyl ether **11**²⁵ (1.468 g, 68%); *R*_f 0.7 (CHCl₃/EtOAc/MeOH (20:5:3)); ¹H NMR (300 MHz, CDCl₃) δ 7.60–7.10 (m, 30H), 6.30–3.00 (m, 41H), 2.20 (m, 1H), 1.30 (m, 1H), 0.83 (s, 9H), 0.01 (s, 6H); ESI-MS *m/z* calcd for C₇₉H₉₇N₅O₂₄Si [M + H]⁺, 1528.63710; found, 1528.8; TOF-HRMS found, 1528.63473.

4',6'-Benzylidene-3',3'',4''-tri-*O*-benzoyl-2''-*O*-carbonylmethyl-5''-*O*-*t*-butyldimethylsilyl-penta-*N*-benzyloxycarbonyl Paromomycin (12). A solution of **11** (5.30 g, 3.46 mmol) in dry pyridine (100 mL) was treated with benzoyl chloride (1.14 mL, 9.812 mmol). The reaction mixture was stirred at room temperature for 16 h. Water (5 mL) was added, and the solvent was removed under vacuum. The residue was dissolved in ethyl acetate, and the organic layer was washed with 0.5 M HCl, satd. NaHCO₃, and water, dried over Na₂SO₄, and concentrated under vacuum. The crude product was purified by silica gel flash chromatography (1:1 EtOAc/hexane) to yield the *O*-benzoyl-protected derivative (5.65 g, quant.); *R*_f 0.6 (1:1 EtOAc/hexane); ¹H NMR (300 MHz, CDCl₃) δ 8.10–7.10 (m, 47H), 6.30–3.00 (m, 44H), 2.20 (m, 1H), 1.30 (m, 1H), 0.83 (s, 9H), 0.01 (s, 6H); ESI-MS *m/z* calcd for C₁₀₀H₁₀₉N₅O₂₇Si [M + H]⁺, 1840.71574; found, 1840.9; TOF-HRMS found, 1840.72060. The compound described above (2.00 g, 1.086 mmol) in CH₂Cl₂ (60 mL) was cooled at –78 °C, and ozone was bubbled for 2 h, after which excess ozone was removed by bubbling argon. The mixture was treated with Me₂S (0.80 mL, 13.816 mmol) and warmed to room temperature, and the solvent was removed under vacuum. The crude solid was purified by silica gel flash chromatography (2:3 EtOAc/hexane) to give the known aldehyde **12**²⁵ (1.627 g, 80%); *R*_f 0.4 (1:1 EtOAc/hexane); ESI-MS *m/z* calcd for C₉₉H₁₀₇N₅O₂₈Si [M + H]⁺, 1842.7; found, 1842.9.

General Procedure for Reductive Amination and Benzoate Deprotection: To a mixture of the aldehyde **12** (80.0 mg, 0.043 mmol) and appropriate amine (0.129 mmol) in dry MeOH (3 mL) was added acetic acid (0.1 mL), followed by NaBH₃CN (1.0 M in THF, 60 μL, 0.060 mmol). A total of 18 h later, a TLC indicated a complete disappearance of the aldehyde. A freshly prepared solution of MeONa/MeOH was added dropwise until the pH reached approximately 10–10.5, and the solution was stirred until a MS analysis indicated that the reaction was finished. This benzoate deprotection needs to be carefully monitored by MS analysis to minimize the formation of a methyl carbamate at the N6''' position. If this undesired product appears in the MS analysis, it is necessary to add more MeOH to dilute the reaction mixture and, therefore, lower the pH at a level where the benzoate esters are cleaved, but with no appreciable amount of methyl carbamate formation at N6'''. When the reaction was finished, the solution was cooled down to –78 °C and dry ice was added until the pH was neutral. Solvent was removed under vacuum, and the residue was taken in EtOAc, washed with water, and dried over Na₂SO₄. After removal of the

solvent under vacuum, the solid was purified by silica gel flash chromatography to obtain the desired amine **13a–z** and **13aa–ah**.

Compounds 13. **Compound 13a:** purified only after AcOH (80%) treatment to remove TBS and benzylidene (67%); silica gel flash chromatography eluent, 5 to 7% MeOH/CH₂Cl₂; *R_f* 0.1 (10% MeOH/CH₂Cl₂); ESI-MS *m/z* calcd for C₇₅H₉₁N₇O₂₆ [M + H]⁺, 1506.6; found, 1506.5. **Compound 13b:** purified only after AcOH (80%) treatment to remove TBS and benzylidene (71%); silica gel flash chromatography eluent, 5 to 7% MeOH/CH₂Cl₂; *R_f* 0.1 (10% MeOH/CH₂Cl₂); ESI-MS *m/z* calcd for C₇₆H₉₃N₇O₂₆ [M + H]⁺, 1520.6; found, 1520.7. **Compound 13c:** 87%; silica gel flash chromatography eluent, 3 to 5% MeOH/CH₂Cl₂; [α]_D +16.6 (c 1.1, MeOH); *R_f* 0.2 (5% MeOH/CH₂Cl₂); ESI-MS *m/z* calcd for C₈₅H₁₀₄N₆O₂₄Si [M + H]⁺, 1621.7; found, 1622.1. **Compound 13d:** 81%; silica gel flash chromatography eluent, 3 to 5% MeOH/CH₂Cl₂; [α]_D +13.8 (c 1.0, MeOH); *R_f* 0.1 (5% MeOH/CH₂Cl₂); ESI-MS *m/z* calcd for C₈₉H₁₁₂N₈O₂₆Si [M + H]⁺, 1737.7; found, 1737.9. **Compound 13e:** 82%; silica gel flash chromatography eluent, 3 to 5% MeOH/CH₂Cl₂; [α]_D +10.9 (c 1.0, MeOH); *R_f* 0.2 (5% MeOH/CH₂Cl₂); ESI-MS *m/z* calcd for C₈₆H₁₀₆N₆O₂₄Si [M + H]⁺, 1635.7; found, 1636.0. **Compound 13f:** purified only after AcOH (80%) treatment to remove TBS and benzylidene; 64%; silica gel flash chromatography eluent, 3 to 5% MeOH/CH₂Cl₂; [α]_D +11.3 (c 0.8, MeOH); *R_f* 0.2 (5% MeOH/CH₂Cl₂); ESI-MS *m/z* calcd for C₇₃H₈₈N₆O₂₄ [M + H]⁺, 1433.6; found, 1433.4. **Compound 13g:** 85%; silica gel flash chromatography eluent, 3 to 5% MeOH/CH₂Cl₂; [α]_D +8.9 (c 1.4, MeOH); *R_f* 0.2 (5% MeOH/CH₂Cl₂); ESI-MS *m/z* calcd for C₈₃H₁₀₁N₇O₂₄Si [M + Na]⁺, 1630.7; found, 1630.8. **Compound 13h:** 78%; silica gel flash chromatography eluent, 3 to 5% MeOH/CH₂Cl₂; [α]_D +10.3 (c 1.1, MeOH); *R_f* 0.15 (5% MeOH/CH₂Cl₂); ESI-MS *m/z* calcd for C₈₅H₁₀₆N₇O₂₄Si [M + H]⁺, 1636.7; found, 1636.8. **Compound 13i:** 79%; silica gel flash chromatography eluent, 3 to 5% MeOH/CH₂Cl₂; [α]_D +15.6 (c 1.2, MeOH); *R_f* 0.2 (5% MeOH/CH₂Cl₂); ESI-MS *m/z* calcd for C₈₇H₁₀₃N₇O₂₄Si [M + H]⁺, 1658.7; found, 1657.7. **Compound 13j:** 87%; silica gel flash chromatography eluent, 3 to 5% MeOH/CH₂Cl₂; [α]_D +17.2 (c 1.3, MeOH); *R_f* 0.1 (5% MeOH/CH₂Cl₂); ESI-MS *m/z* calcd for C₈₉H₁₁₂N₈O₂₆Si [M + H]⁺, 1737.8; found, 1738.2. **Compound 13k:** 85%; silica gel flash chromatography eluent, 3 to 5% MeOH/CH₂Cl₂; [α]_D +10.4 (c 0.8, MeOH); *R_f* 0.2 (5% MeOH/CH₂Cl₂); ESI-MS *m/z* calcd for C₈₃H₁₀₁N₇O₂₄Si [M + H]⁺, 1608.7; found, 1608.8. **Compound 13l:** purified only after AcOH (80%) treatment to remove TBS and benzylidene; 67%; silica gel flash chromatography eluent, 6 to 8% MeOH/CH₂Cl₂; [α]_D +7.3 (c 1.6, MeOH); *R_f* 0.2 (10% MeOH/CH₂Cl₂); ESI-MS *m/z* calcd for C₇₃H₈₆N₈O₂₄ [M + H]⁺, 1459.6; found, 1459.7. **Compound 13m:** 82%; silica gel flash chromatography eluent, 3 to 5% MeOH/CH₂Cl₂; [α]_D +21.3 (c 1.2, MeOH); *R_f* 0.2 (5% MeOH/CH₂Cl₂); ESI-MS *m/z* calcd for C₈₄H₁₀₂N₆O₂₄Si [M + H]⁺, 1607.7; found, 1608.9. **Compound 13n:** 78%; silica gel flash chromatography eluent, 3 to 5% MeOH/CH₂Cl₂; [α]_D +6.3 (c 0.7, MeOH); *R_f* 0.15 (5% MeOH/CH₂Cl₂); ESI-MS *m/z* calcd for C₈₅H₁₀₄N₆O₂₄Si [M + H]⁺, 1621.7; found, 1621.8. **Compound 13o:** 90%; silica gel flash chromatography eluent, 3 to 5% MeOH/CH₂Cl₂; [α]_D +14.7 (c 1.0, MeOH); *R_f* 0.2 (5% MeOH/CH₂Cl₂); ESI-MS *m/z* calcd for C₈₇H₁₀₈N₆O₂₄Si [M + Na]⁺, 1671.7; found, 1671.9. **Compound 13p:** 86%; silica gel flash chromatography eluent, 3 to 5% MeOH/CH₂Cl₂; [α]_D +12.8 (c 0.9, MeOH); *R_f* 0.2 (5% MeOH/CH₂Cl₂); ESI-MS *m/z* calcd for C₈₈H₁₁₀N₆O₂₄Si [M + Na]⁺, 1685.7; found, 1686.1. **Compound 13q:** 83%; silica gel flash chromatography eluent, 3 to 5% MeOH/CH₂Cl₂; [α]_D +8.4 (c 0.8, MeOH); *R_f* 0.2 (5% MeOH/CH₂Cl₂); ESI-MS *m/z* calcd for C₈₇H₁₀₈N₆O₂₅Si [M + H]⁺, 1665.7; found, 1665.6. **Compound 13r:** 94%; silica gel flash chromatography eluent, 3 to 5% MeOH/CH₂Cl₂; [α]_D +13.8 (c 0.8, MeOH); *R_f* 0.2 (5% MeOH/CH₂Cl₂); ESI-MS *m/z* calcd for C₈₇H₁₀₅F₃N₆O₂₄Si [M + H]⁺, 1703.7; found, 1703.5. **Compound 13s:** 81%; silica gel flash chromatography eluent, 3 to 5% MeOH/CH₂Cl₂; [α]_D +11.7 (c 0.8, MeOH); *R_f* 0.15 (5% MeOH/CH₂Cl₂); ESI-MS *m/z* calcd for C₉₂H₁₁₀N₆O₂₄Si [M + H]⁺, 1711.7; found, 1711.7. **Compound 13t:** 84%; silica gel flash chromatography eluent, 3 to 5% MeOH/CH₂Cl₂; [α]_D +14.9 (c 1.0, MeOH); *R_f* 0.15

(5% MeOH/CH₂Cl₂); ESI-MS *m/z* calcd for C₈₈H₁₁₀N₆O₂₆Si [M + H]⁺, 1695.7; found, 1695.9. **Compound 13u:** 85%; silica gel flash chromatography eluent, 3 to 5% MeOH/CH₂Cl₂; [α]_D +14.6 (c 1.1, MeOH); *R_f* 0.2 (5% MeOH/CH₂Cl₂); ESI-MS *m/z* calcd for C₈₈H₁₀₄F₆N₆O₂₄Si [M + H]⁺, 1771.7; found, 1771.5. **Compound 13v:** 87%; silica gel flash chromatography eluent, 3 to 5% MeOH/CH₂Cl₂; [α]_D +12.7 (c 0.9, MeOH); *R_f* 0.2 (5% MeOH/CH₂Cl₂); ESI-MS *m/z* calcd for C₉₀H₁₀₈N₆O₂₄Si [M + H]⁺, 1684.7; found, 1685.8. **Compound 13w:** 78%; silica gel flash chromatography eluent, 3 to 5% MeOH/CH₂Cl₂; [α]_D +17.3 (c 1.2, MeOH); *R_f* 0.1 (5% MeOH/CH₂Cl₂); ESI-MS *m/z* calcd for C₈₄H₁₀₂N₆O₂₅Si [M + H]⁺, 1623.7; found, 1623.8. **Compound 13x:** 80%; silica gel flash chromatography eluent, 3 to 5% MeOH/CH₂Cl₂; [α]_D +15.6 (c 1.0, MeOH); *R_f* 0.2 (5% MeOH/CH₂Cl₂); ESI-MS *m/z* calcd for C₈₈H₁₀₈N₆O₂₄Si [M + H]⁺, 1661.7; found, 1661.6. **Compound 13y:** 80%; silica gel flash chromatography eluent, 3 to 5% MeOH/CH₂Cl₂; [α]_D +5.7 (c 0.8, MeOH); *R_f* 0.1 (5% MeOH/CH₂Cl₂); ESI-MS *m/z* calcd for C₈₄H₁₀₈N₆O₂₄Si [M + H]⁺, 1613.7; found, 1614.9. **Compound 13z:** 73%; silica gel flash chromatography eluent, 3 to 5% MeOH/CH₂Cl₂; [α]_D +13.7 (c 1.0, MeOH); *R_f* 0.2 (5% MeOH/CH₂Cl₂); ESI-MS *m/z* calcd for C₈₇H₁₁₂N₆O₂₄Si [M + H]⁺, 1653.8; found, 1653.7. **Compound 13aa:** 91%; silica gel flash chromatography eluent, 3 to 5% MeOH/CH₂Cl₂; [α]_D +14.3 (c 1.0, MeOH); *R_f* 0.1 (5% MeOH/CH₂Cl₂); ESI-MS *m/z* calcd for C₈₈H₁₁₂N₆O₂₅Si [M + H]⁺, 1681.8; found, 1681.6. **Compound 13ab:** 72%; silica gel flash chromatography eluent, 3 to 5% MeOH/CH₂Cl₂; [α]_D +16.9 (c 1.2, MeOH); *R_f* 0.1 (5% MeOH/CH₂Cl₂); ESI-MS *m/z* calcd for C₈₄H₁₁₀N₆O₂₄Si [M + H]⁺, 1615.7; found, 1615.8. **Compound 13ac:** 87%; silica gel flash chromatography eluent, 3 to 4% MeOH/CH₂Cl₂; [α]_D +12.2 (c 1.0, MeOH); *R_f* 0.3 (5% MeOH/CH₂Cl₂); ESI-MS *m/z* calcd for C₁₀₅H₁₄₄N₆O₂₄Si [M + H]⁺, 1902.0; found, 1902.2. **Compound 13ad:** 75%; silica gel flash chromatography eluent, 3 to 5% MeOH/CH₂Cl₂; [α]_D +11.8 (c 0.8, MeOH); *R_f* 0.1 (5% MeOH/CH₂Cl₂); ESI-MS *m/z* calcd for C₉₂H₁₀₇N₇O₂₆Si [M + H]⁺, 1754.7; found, 1755.7. **Compound 13ae:** 91%; silica gel flash chromatography eluent, 3 to 5% MeOH/CH₂Cl₂; [α]_D +10.9 (c 0.8, MeOH); *R_f* 0.2 (5% MeOH/CH₂Cl₂); ESI-MS *m/z* calcd for C₈₀H₁₀₂N₆O₂₄Si [M + H]⁺, 1559.7; found, 1560.5. **Compound 13af:** 88%; silica gel flash chromatography eluent, 3 to 4% MeOH/CH₂Cl₂; [α]_D +15.2 (c 1.0, MeOH); *R_f* 0.3 (5% MeOH/CH₂Cl₂); ESI-MS *m/z* calcd for C₉₅H₁₁₈N₆O₂₄Si [M + H]⁺, 1753.8; found, 1754.1. **Compound 13ag:** 85%; silica gel flash chromatography eluent, 3% MeOH/CH₂Cl₂; [α]_D +21.7 (c 1.1, MeOH); *R_f* 0.4 (5% MeOH/CH₂Cl₂); ESI-MS *m/z* calcd for C₉₄H₁₃₀N₆O₂₄Si [M + H]⁺, 1755.9; found, 1756.3. **Compound 13ah:** 89%; silica gel flash chromatography eluent, 3 to 5% MeOH/CH₂Cl₂; [α]_D +17.6 (c 0.4, MeOH); *R_f* 0.3 (5% MeOH/CH₂Cl₂); ESI-MS *m/z* calcd for C₉₀H₁₁₄N₇O₂₆Si [M + H]⁺, 1734.7; found, 1735.1.

General Procedure for Final Deprotection: The appropriate substrate was dissolved in 80% aqueous acetic acid (3 mL), and the solution was heated at 60 °C for 2–5 h or until a MS analysis showed total conversion of the starting material into the benzylidene as well as TBS deprotected product. The solution was cooled down to room temperature, a catalytic amount of 20% palladium hydroxide on carbon was added, and the suspension was stirred at room temperature under an atmosphere of hydrogen (hydrogen balloon) until the conversion of the starting material into the product was completed as indicated by MS analysis. The mixture was filtered through a layer of Celite on cotton, concentrated under vacuum, washed with CH₂Cl₂ twice, and lyophilized to afford compounds **5–9**, **9a,b**, **14a–z**, and **14aa–ae** as per acetate salts.

Compounds 5–9. **Compound 5:** 75%; [α]_D +8.8 (c 0.6, H₂O); ¹H NMR (400 MHz, D₂O) δ 5.75 (m, 1H), 5.44 (m, 1H), 5.20 (m, 1H), 4.30–4.00 (m, 6H), 3.85–3.50 (m, 12H), 3.40–3.15 (m, 6H), 3.00–2.55 (m, 6H) 2.31 (m, 1H), 1.91 (s, 21H), 1.63 (m, 1H); ¹³C NMR (125 MHz, D₂O) δ 181.9, 109.8, 96.7, 96.3, 86.2, 81.5, 81.0, 75.3, 73.8, 73.3, 70.9, 70.4, 69.7, 68.4, 67.9, 61.2, 60.6, 60.4, 54.7, 51.6, 50.7, 49.9, 41.4, 39.4, 31.9, 32.7, 28.5, 28.1, 23.7; ESI-MS *m/z* calcd for C₂₇H₃₅N₇O₁₄ [M + H]⁺, 701.38852; found, 702.4; TOF-HRMS found, 702.38698. **Compound 6:** 80%; [α]_D +5.7 (c

0.4, H₂O); ¹H NMR (400 MHz, D₂O) δ 5.72 (m, 1H), 5.44 (m, 1H), 5.21 (m, 1H), 4.59 (m, 1H), 4.20–4.00 (m, 5H), 3.95–3.50 (m, 12H), 3.45–2.7 (m, 14H), 2.26 (m, 1H), 1.87 (s, 21H), 1.59 (m, 1H); ¹³C NMR (125 MHz, D₂O) δ 182.2, 108.9, 96.8, 96.0, 86.0, 81.8, 79.8, 74.5, 74.3, 71.3, 71.2, 70.1, 68.6, 68.2, 67.5, 61.0, 54.8, 51.8, 51.1, 50.3, 49.8, 48.8, 45.5, 43.7, 41.1, 37.3, 31.1, 27.4, 24.5, 24.0; ESI-MS *m/z* calcd for C₂₈H₅₇N₇O₁₄ [M + H]⁺, 716.40417; found, 716.4; TOF-HRMS found, 716.40380. **Compound 7:** 80%; [α]_D +5.4 (c 0.6, H₂O); ¹H NMR (400 MHz, D₂O) δ 8.40–8.32 (m, 2H), 7.70–7.30 (m, 2H), 5.71 (m, 1H), 5.38 (m, 1H), 5.16 (m, 1H), 4.55 (m, 1H), 4.20–4.00 (m, 7H), 3.95–3.50 (m, 12H), 3.45–3.15 (m, 8H), 2.32 (m, 1H), 1.81 (s, 21H), 1.60 (m, 1H); ¹³C NMR (125 MHz, D₂O) δ 181.4, 150.5, 140.0, 132.8, 129.8, 125.5, 109.0, 96.6, 95.7, 85.7, 81.4, 78.5, 74.3, 73.7, 71.1, 70.3, 69.9, 69.3, 68.5, 68.1, 67.5, 66.3, 61.0, 60.1, 54.6, 51.6, 50.8, 49.6, 46.6, 43.5, 41.1, 29.7, 23.5; ESI-MS *m/z* calcd for C₃₁H₅₅N₇O₁₄ [M + H]⁺, 750.38852; found, 750.4; TOF-HRMS found, 750.38473. **Compound 8:** 70%; [α]_D +10.6 (c 0.6, H₂O); ¹H NMR (400 MHz, D₂O) δ 7.82 (s, 1H), 7.66 (d, 5 Hz, 1H), 6.76 (d, 5 Hz, 1H), 5.69 (m, 1H), 5.32 (m, 1H), 5.12 (m, 1H), 4.50 (m, 1H), 4.14–4.04 (m, 5H), 3.85–3.50 (m, 12H), 3.13–3.17 (m, 10H), 2.31 (m, 1H), 1.91 (s, 21H), 1.65 (m, 1H); ¹³C NMR (125 MHz, D₂O) δ 180.1, 156.7, 143.5, 142.1, 116.2, 113.0, 108.5, 96.2, 95.1, 85.1, 81.0, 80.9, 77.2, 74.1, 73.8, 72.9, 70.7, 69.4, 69.1, 68.0, 67.5, 66.8, 66.0, 60.5, 59.5, 54.1, 51.1, 49.0, 47.9, 46.7, 40.6, 28.6, 22.6; ESI-MS *m/z* calcd for C₃₁H₅₆N₈O₁₄ [M + H]⁺, 765.39942; found, 765.7; TOF-HRMS *m/z* calcd for C₃₁H₅₆N₈O₁₄ [M + Na]⁺, 787.38137; found, 787.38206. **Compound 9:** 80%; [α]_D +8.3 (c 0.5, H₂O); ¹H NMR (400 MHz, D₂O) δ 7.22 (m, 5H), 5.68 (m, 1H), 5.32 (m, 1H), 5.11 (m, 1H), 4.52 (m, 1H), 4.15–4.05 (m, 5H), 3.90–3.54 (m, 12H), 3.35–3.17 (m, 10H), 2.71 (m, 2H), 2.29 (m, 1H), 1.93 (s, 18H), 1.67 (m, 1H); ¹³C NMR (125 MHz, D₂O) δ 180.9, 136.6, 129.4 (2C), 129.1 (2C), 127.8, 108.5, 96.2, 95.1, 85.2, 80.9, 80.8, 77.6, 74.0, 73.7, 73.5, 73.0, 70.7, 69.8, 69.4, 68.0, 67.6, 65.7, 60.5, 59.5, 54.1, 51.1, 49.0, 48.7, 47.2, 46.7, 40.6, 29.0, 23.2; ESI-MS *m/z* calcd for C₃₃H₅₈N₆O₁₄ [M + H]⁺, 762.4011; found, 763.4; TOF-HRMS found, 763.40657. **Compound 9a:** 76%; [α]_D +9.4 (c 0.6, H₂O); ¹H NMR (400 MHz, D₂O) δ 7.25 (m, 5H), 5.66 (m, 1H), 5.33 (m, 1H), 5.11 (m, 1H), 4.55 (m, 1H), 4.14–2.0–4.05 (m, 5H), 3.85–3.45 (m, 12H), 3.37–3.22 (m, 8H), 2.95 (m, 2H), 2.31 (m, 1H), 1.99–1.88 (s, 18H), 1.69 (m, 1H); ESI-MS *m/z* calcd for C₃₅H₆₀N₆O₁₅ [M + H]⁺, 805.41949; found, 805.6; TOF-HRMS found, 805.41607. **Compound 9b:** 70%; [α]_D +8.7 (c 0.5, H₂O); ¹H NMR (400 MHz, D₂O) δ 7.79 (m, 2H), 7.46–7.35 (m, 3H), 7.24 (m, 5H), 5.69 (m, 1H), 5.31 (m, 1H), 5.12 (m, 1H), 4.54 (m, 1H), 4.15–4.00 (m, 5H), 3.85–3.50 (m, 12H), 3.35–3.21 (m, 8H), 2.91 (m, 2H), 2.30 (m, 1H), 1.91 (s, 15H), 1.67 (m, 1H); ESI-MS *m/z* calcd for C₃₅H₆₀N₆O₁₅ [M + H]⁺, 867.43514; found, 867.8; TOF-HRMS found, 867.43400.

Compounds 14. **Compound 14a:** 78%; [α]_D +10.6 (c 0.7, H₂O); ¹H NMR (400 MHz, D₂O) δ 5.78 (m, 1H), 5.46 (m, 1H), 5.26 (m, 1H), 4.30–4.00 (m, 6H), 3.95–3.50 (m, 14H), 3.45–3.00 (m, 6H), 2.35 (m, 1H), 1.91 (s, 18H), 1.71 (m, 1H); ¹³C NMR (125 MHz, D₂O) δ 181.7, 110.2, 97.3, 95.7, 86.2, 82.3, 77.8, 76.0, 74.7, 73.9, 72.6, 70.8, 69.4, 69.3, 68.2, 67.6, 61.4, 60.5, 58.8, 54.9, 52.6, 52.1, 49.3, 48.1, 42.3, 27.6, 23.4; ESI-MS *m/z* calcd for C₂₅H₅₀N₆O₁₄ [M + H]⁺, 659.34633; found, 659.4; TOF-HRMS found, 659.34410. **Compound 14b:** 70%; [α]_D +7.8 (c 1.0, H₂O); ¹H NMR (400 MHz, D₂O) δ 5.66 (m, 1H), 5.30 (m, 1H), 5.11 (m, 1H), 4.46 (m, 1H), 4.20–4.00 (m, 5H), 3.95–3.50 (m, 14H), 3.40–2.95 (m, 11H), 2.37 (m, 1H), 2.1–1.9 (m, 4H), 1.79 (s, 21H), 1.70 (m, 1H); ¹³C NMR (125 MHz, D₂O) δ 181.0, 108.9, 96.6, 95.7, 90.9, 85.5, 81.5, 77.7, 74.5, 74.3, 73.3, 71.1, 69.9, 69.5, 68.4, 68.3, 68.0, 61.0, 54.5, 52.4, 51.5, 50.6, 49.4, 44.7, 44.2, 41.0, 40.1, 34.5, 28.9, 23.3, 20.9, 20.2; ESI-MS *m/z* calcd for C₃₀H₅₉N₇O₁₄ [M + H]⁺, 741.41982; found, 742.7; TOF-HRMS found, 742.41783. **Compound 14c:** 75%; [α]_D +12.4 (c 1.1, H₂O); ¹H NMR (400 MHz, D₂O) δ 5.67 (m, 1H), 5.32 (m, 1H), 5.25 (m, 1H), 4.48 (m, 1H), 4.20–4.00 (m, 5H), 3.95–3.30 (m, 14H), 3.30–2.75 (m, 13H), 2.21 (m, 1H), 1.81 (s, 21H), 1.72 (m, 1H), 1.63–1.45 (m, 4H); ¹³C NMR (125 MHz, D₂O) δ 180.3, 108.5, 96.2, 95.2, 85.0, 81.1, 80.8, 77.2, 74.1, 72.9,

70.7, 69.4, 69.1, 67.9, 67.5, 60.5, 60.1, 54.1, 51.1, 50.3, 50.2, 49.1, 48.9, 46.1, 44.2, 44.1, 40.6, 30.3, 28.6, 22.7, 22.1, 21.4, 18.2; ESI-MS *m/z* calcd for C₃₁H₆₁N₇O₁₄ [M + H]⁺, 756.43547; found, 756.7; TOF-HRMS found, 756.43313. **Compound 14d:** 75%; [α]_D +6.8 (c 0.4, H₂O); ¹H NMR (400 MHz, D₂O) δ 8.00–7.70 (m, 2H), 7.60–7.40 (m, 2H), 5.70 (m, 1H), 5.33 (m, 1H), 5.11 (m, 1H), 4.50 (m, 1H), 4.20–4.00 (m, 5H), 3.85–3.50 (m, 14H), 3.40–3.15 (m, 6H), 2.37 (m, 1H), 1.79 (s, 21H), 1.70 (m, 1H); ¹³C NMR (125 MHz, D₂O) δ 181.4, 132.3, 131.6, 129.5, 128.7, 126.8, 108.8, 96.2, 95.3, 85.3, 81.6, 81.0, 78.0, 74.1, 73.1, 71.5, 70.7, 69.6, 69.3, 68.0, 67.7, 60.7, 60.3, 54.2, 51.5, 51.1, 50.3, 49.2, 43.0, 40.7, 29.2, 23.5; ESI-MS *m/z* calcd for C₃₀H₅₃N₇O₁₄ [M + H]⁺, 736.37287; found, 736.5; TOF-HRMS found, 736.37359. **Compound 14e:** 70%; [α]_D +7.6 (c 0.4, H₂O); ¹H NMR (400 MHz, D₂O) δ 8.41–8.42 (m, 2H), 7.92 (d, *J* = 4.4 Hz, 1H), 7.52 (m, 1H), 5.69 (m, 1H), 5.33 (m, 1H), 5.13 (m, 1H), 4.50 (m, 1H), 4.20–4.00 (m, 7H), 3.90–3.52 (m, 12H), 3.41–3.02 (m, 10H), 2.33 (m, 1H), 1.99 (m, 1H), 1.84 (s, 21H); ¹³C NMR (125 MHz, D₂O) δ 179.7, 146.9, 141.8, 134.5, 130.1, 126.2, 109.0, 96.7, 95.6, 85.6, 81.3, 77.7, 74.6, 74.3, 73.4, 71.2, 70.4, 69.9, 69.5, 68.4, 68.0, 67.4, 66.2, 61.0, 60.0, 54.5, 51.6, 50.7, 49.5, 48.4, 47.9, 41.1, 29.4, 22.5; ESI-MS *m/z* calcd for C₃₂H₅₇N₇O₁₄ [M + H]⁺, 764.40417; found, 764.7; TOF-HRMS found, 764.40547. **Compound 14f:** 80%; [α]_D +7.5 (c 0.2, H₂O); ¹H NMR (400 MHz, D₂O) δ 8.42 (m, 1H), 7.85 (m, 2H), 7.41 (m, 3H), 5.72 (m, 1H), 5.38 (m, 1H), 5.17 (m, 1H), 4.55 (m, 1H), 4.20–4.00 (m, 5H), 3.95–3.50 (m, 12H), 3.45–3.15 (m, 8H), 2.32 (m, 1H), 1.81 (s, 21H), 1.65–1.40 (m, 1H); ¹³C NMR (125 MHz, D₂O) δ 181.8, 143.4, 140.5, 138.4, 130.2, 129.6, 127.3, 126.9, 122.5, 114.6, 109.1, 96.5, 95.6, 85.1, 81.8, 78.5, 75.6, 74.4, 72.8, 70.1, 69.9, 69.6, 68.3, 67.5, 60.9, 60.4, 54.5, 52.6, 51.5, 50.4, 49.5, 41.0, 29.2, 28.0, 23.8; ESI-MS *m/z* calcd for C₃₄H₅₅N₇O₁₄ [M + H]⁺, 786.38852; found, 786.5; TOF-HRMS found, 786.38421. **Compound 14g:** 75%; [α]_D +5.6 (c 0.3, H₂O); ¹H NMR (400 MHz, D₂O) δ 7.91 (m, 1H), 7.45 (m, 1H), 6.65 (m, 1H), 5.67 (m, 1H), 5.32 (m, 1H), 5.10 (m, 1H), 4.51 (m, 1H), 4.15–4.00 (m, 5H), 3.76–3.50 (m, 12H), 3.41–3.16 (m, 10H), 2.32 (m, 1H), 1.81 (s, 21H), 1.65–1.50 (m, 1H); ¹³C NMR (125 MHz, D₂O) δ 180.8, 157.6, 116.31, 142.7, 136.2, 112.3, 108.5, 96.2, 95.1, 85.2, 82.1, 81.1, 80.8, 77.5, 74.0, 73.8, 73.0, 70.7, 69.4, 69.2, 67.9, 67.6, 65.5, 60.5, 59.5, 54.1, 51.1, 50.3, 49.0, 46.6, 40.6, 28.8, 23.2; ESI-MS *m/z* calcd for C₃₁H₅₆N₈O₁₄ [M + H]⁺, 765.39942; found, 765.6; TOF-HRMS found, 765.39871. **Compound 14h:** 80%; [α]_D +9.7 (c 0.5, H₂O); ¹H NMR (400 MHz, D₂O) δ 7.78 (m, 1H), 7.31 (m, 1H), 6.94 (m, 1H), 6.79 (m, 1H), 5.72 (m, 1H), 5.34 (m, 1H), 5.10 (m, 1H), 4.51 (m, 1H), 4.21–4.06 (m, 5H), 3.90–3.46 (m, 14H), 3.39–3.22 (m, 6H), 2.37 (m, 1H), 1.81 (s, 21H), 1.68 (m, 1H); ¹³C NMR (125 MHz, D₂O) δ 180.9, 154.1, 144.2, 136.3, 129.6, 113.5, 109.1, 96.5, 95.5, 85.6, 81.7, 81.3, 77.6, 74.6, 74.1, 73.3, 71.1, 69.9, 69.5, 68.4, 68.3, 68.1, 61.0, 60.4, 54.5, 51.6, 50.6, 49.5, 42.4, 41.1, 29.1, 23.3; ESI-MS *m/z* calcd for C₃₀H₅₃N₇O₁₄ [M + H]⁺, 736.37287; found, 736.5; TOF-HRMS found, 736.37085. **Compound 14i:** 75%; [α]_D +8.6 (c 0.6, H₂O); ¹H NMR (400 MHz, D₂O) δ 7.80–7.40 (m, 4H), 5.81 (m, 1H), 5.44 (m, 1H), 5.24 (m, 1H), 4.35–4.10 (m, 6H), 3.95–3.50 (m, 14H), 3.45–3.15 (m, 8H), 2.42 (m, 1H), 1.91 (s, 21H), 1.61 (m, 1H); ESI-MS *m/z* calcd for C₃₃H₅₆N₈O₁₄ [M + H]⁺, 789.39942; found, 789.5; TOF-HRMS found, 789.39932. **Compound 14j:** 80%; [α]_D +6.7 (c 0.5, H₂O); ¹H NMR (400 MHz, D₂O) δ 7.22–6.91 (m, 5H), 5.65 (m, 1H), 5.25 (m, 1H), 5.16 (m, 1H), 4.41 (m, 1H), 4.25–4.05 (m, 5H), 3.91–3.55 (m, 12H), 3.44–3.20 (m, 8H), 2.33 (m, 1H), 1.80 (s, 18H), 1.72 (m, 1H); ¹³C NMR (125 MHz, D₂O) δ 180.9, 144.7, 129.1 (2C), 119.6, 116.3 (2C), 109.5, 95.7, 94.8, 84.1, 80.7, 78.1, 74.5, 74.6, 73.2, 72.8, 72.2, 69.8, 69.5, 68.7, 68.6, 67.2, 66.8, 59.8, 59.5, 53.5, 50.4, 49.5, 48.4, 40.0, 28.8, 22.8; ESI-MS *m/z* calcd for C₃₁H₅₄N₆O₁₄ [M + H]⁺, 735.37763; found, 735.5; TOF-HRMS found, 735.37748. **Compound 14k:** 85%; [α]_D +8.5 (c 0.4, H₂O); ¹H NMR (400 MHz, D₂O) δ 7.33 (m, 5H), 5.67 (m, 1H), 5.32 (m, 1H), 5.08 (m, 1H), 4.48 (m, 1H), 4.16–4.01 (m, 5H), 3.89–3.48 (m, 14H), 3.36–3.16 (m, 8H), 2.31 (m, 1H), 1.91 (s, 18H), 1.65 (m, 1H); ¹³C NMR (125 MHz, D₂O) δ 181.5, 131.2, 130.7 (2C), 130.1 (2C), 129.6, 108.9, 96.6, 95.6, 85.6, 81.6, 78.1, 74.5, 74.3,

73.5, 71.2, 69.9, 69.6, 68.4, 68.0, 66.2, 60.9, 60.1, 54.6, 51.8, 51.6, 50.7, 49.5, 47.1, 41.1, 40.1, 29.5, 23.6; ESI-MS m/z calcd for $C_{32}H_{56}N_6O_{14}$ [M + H]⁺, 749.39328; found, 749.6; TOF-HRMS found, 749.39319. **Compound 14l**: 90%; [α]_D +11.4 (c 0.4, H₂O); ¹H NMR (400 MHz, D₂O) δ 7.27 (m, 5H), 5.74 (m, 1H), 5.36 (m, 1H), 5.27 (m, 1H), 4.29 (m, 1H), 4.21–4.07 (m, 5H), 3.90–3.14 (m, 22H), 2.70–2.61 (m, 2H), 2.32 (m, 1H), 2.21 (m, 2H), 1.89 (s, 18H), 1.61 (m, 1H); ¹³C NMR (125 MHz, D₂O) δ 182.3, 132.8, 129.5 (2C), 129.3 (2C), 126.9, 110.5, 97.6, 97.0, 85.6, 82.0, 81.8, 76.0, 74.5, 74.2, 74.0, 71.3, 71.1, 70.2, 69.1, 68.4, 61.7, 61.1, 55.2, 52.0, 51.2, 50.1, 41.3, 39.7, 33.2, 32.6, 30.7, 29.7, 28.7, 24.1; ESI-MS m/z calcd for $C_{34}H_{60}N_6O_{14}$ [M + H]⁺, 777.42458; found, 777.6; TOF-HRMS found, 777.42090. **Compound 14m**: 90%; [α]_D +9.6 (c 0.5, H₂O); ¹H NMR (400 MHz, D₂O) δ 7.22 (m, 5H), 5.55 (m, 1H), 5.27 (m, 1H), 5.14 (m, 1H), 4.45 (m, 1H), 4.25–4.08 (m, 5H), 3.81–2.94 (m, 22H), 2.61 (m, 2H), 2.31–2.15 (m, 3H), 1.79 (s, 18H), 1.4–1.65 (m, 3H); ¹³C NMR (125 MHz, D₂O) δ 181.8, 143.2, 128.9 (4C), 126.3, 110.1, 96.9, 96.3, 85.2, 81.5, 81.1, 75.4, 73.9, 73.7, 73.6, 70.7, 70.3, 69.7, 68.4, 67.8, 61.2, 60.6, 60.4, 54.7, 51.4, 50.7, 49.6, 40.8, 39.4, 34.9, 31.8, 32.7, 28.3, 28.1, 23.6; ESI-MS m/z calcd for $C_{35}H_{62}N_6O_{14}$ [M + H]⁺, 791.44023; found, 791.7; TOF-HRMS found, 791.44394. **Compound 14n**: 90%; [α]_D +5.4 (c 0.2, H₂O); ¹H NMR (400 MHz, D₂O) δ 7.13 (s, 2H), 6.85 (m, 2H), 5.66 (m, 1H), 5.26 (m, 1H), 5.17 (m, 1H), 4.42 (m, 1H), 4.14–2.8–4.08 (m, 5H), 3.88–3.56 (m, 15H), 3.46–3.20 (m, 10H), 2.81 (m, 2H), 2.34 (m, 1H), 1.79 (s, 18H), 1.72 (m, 1H); ¹³C NMR (125 MHz, D₂O) δ 182.2, 158.7, 130.9 (2C), 115.2 (2C), 110.5, 97.5, 96.8, 85.5, 82.0, 81.8, 75.9, 74.4, 74.1, 72.5, 71.2, 70.9, 70.2, 69.0, 68.3, 66.3, 61.1, 61.0, 56.1, 55.9, 55.2, 52.0, 51.2, 50.3, 41.5, 32.6, 32.1, 24.1; ESI-MS m/z calcd for $C_{34}H_{60}N_6O_{15}$ [M + H]⁺, 793.41949; found, 793.7; TOF-HRMS found, 793.41776. **Compound 14o**: 85%; [α]_D +6.5 (c 0.2, H₂O); ¹H NMR (400 MHz, D₂O) δ 7.57 (s, 2H), 7.35 (m, 2H), 5.66 (m, 1H), 5.25 (m, 1H), 5.16 (m, 1H), 4.41 (m, 1H), 4.14–2.9–4.06 (m, 5H), 3.87–3.56 (m, 12H), 3.47–3.15 (m, 10H), 2.94 (m, 2H), 2.33 (m, 1H), 1.79 (s, 18H), 1.68 (m, 1H); ¹³C NMR (125 MHz, D₂O) δ 182.2, 141.7, 130.1, 126.5, 110.2, 98.4, 97.8, 85.2, 82.4, 82.0, 76.0, 75.2, 74.1, 74.0, 72.4, 71.9, 71.5, 70.3, 69.8, 68.7, 67.2, 61.2, 55.5, 59.8, 52.3, 51.2, 50.3, 41.3, 41.0, 36.7, 33.4 24.1; ESI-MS m/z calcd for $C_{34}H_{57}F_3N_6O_{14}$ [M + H]⁺, 831.39631; found, 831.5; TOF-HRMS found, 831.39758. **Compound 14p**: 85%; [α]_D +10.8 (c 0.6, H₂O); ¹H NMR (400 MHz, D₂O) δ 7.57 (m, 2H), 7.42 (m, 2H), 7.31 (m, 5H), 5.69 (m, 1H), 5.32 (m, 1H), 5.12 (m, 1H), 4.5 (m, 1H), 4.14–4.04 (m, 5H), 3.85–3.50 (m, 12H), 3.30–3.17 (m, 10H), 2.78 (m, 2H), 2.31 (m, 1H), 1.91 (s, 18H), 1.65 (m, 1H); ¹³C NMR (125 MHz, D₂O) δ 181.2, 138.4, 136.1, 132.7 (2C), 130.9 (2C), 130.0 (2C), 128.4, 127.1 (2C), 126.3, 109.1, 97.6, 95.4, 87.1, 81.5, 80.6, 78.1, 74.8, 74.1, 73.9, 73.4, 71.2, 70.1, 69.4, 68.6, 67.9, 65.7, 60.7, 59.3, 54.7, 53.2, 50.8, 49.4, 48.0, 46.9, 41.5, 29.3, 23.8; ESI-MS m/z calcd for $C_{39}H_{62}N_6O_{14}$ [M + H]⁺, 839.44023; found, 839.5; TOF-HRMS found, 839.43844. **Compound 14q**: 90%; [α]_D +11.4 (c 0.7, H₂O); ¹H NMR (400 MHz, D₂O) δ 6.40 (m, 3H), 5.67 (m, 1H), 5.24 (m, 1H), 5.15 (m, 1H), 4.41 (m, 1H), 4.28–4.07 (m, 5H), 3.90–3.55 (m, 18H), 3.46–3.11 (m, 10H), 2.82 (m, 2H), 2.34 (m, 1H), 1.79 (s, 18H), 1.67 (m, 1H); ¹³C NMR (125 MHz, D₂O) δ 181.0, 160.0 (2C), 138.9, 109.4, 106.8 (2C), 98.6, 96.1, 95.3, 84.3, 80.6, 80.2, 74.5, 73.0, 72.8, 71.9, 71.4, 69.9, 69.4, 68.9, 67.6, 67.0, 61.3, 59.8, 59.6, 55.0, 53.8, 50.6, 49.9, 48.7, 40.0, 32.4, 30.8, 22.8; ESI-MS m/z calcd for $C_{35}H_{62}N_6O_{16}$ [M + H]⁺, 823.43006; found, 823.5; TOF-HRMS found, 823.42847. **Compound 14r**: 90%; [α]_D +5.6 (c 0.3, H₂O); ¹H NMR (400 MHz, D₂O) δ 7.72 (m, 1H), 7.65 (m, 2H), 5.66 (m, 1H), 5.26 (m, 1H), 5.17 (m, 1H), 4.42 (m, 1H), 4.14–2.8–4.08 (m, 5H), 3.88–3.56 (m, 12H), 3.46–3.20 (m, 10H), 2.94 (m, 2H), 2.34 (m, 1H), 1.79 (s, 24H), 1.72 (m, 1H); ESI-MS m/z calcd for $C_{35}H_{56}F_6N_6O_{14}$ [M + H]⁺, 899.38369; found, 899.4; TOF-HRMS found, 899.38216. **Compound 14s**: 80%; [α]_D +9.2 (c 0.5, H₂O); ¹H NMR (400 MHz, D₂O) δ 7.82 (m, 3H), 7.66 (m, 1H), 7.47 (m, 2H), 7.34 (m, 1H), 5.68 (m, 1H), 5.32 (m, 1H), 5.11 (m, 1H), 4.52 (m, 1H), 4.15–4.05 (m, 5H), 3.90–3.54 (m, 12H), 3.35–3.17 (m, 10H), 2.81 (m, 2H), 2.29 (m, 1H), 1.93 (s, 18H), 1.67 (m, 1H); ¹³C NMR (125 MHz, D₂O) δ

182.1, 136.6, 131.7, 130.9, 130.2, 129.7, 129.3, 128.7, 128.2, 127.8, 124.7, 109.6, 97.1, 96.3, 84.3, 81.7, 81.2, 78.2, 74.3, 74.0, 73.6, 73.2, 71.2, 70.4, 69.8, 68.5, 68.0, 66.2, 60.7, 60.1, 54.6, 51.7, 49.5, 49.1, 48.0, 46.9, 41.4, 31.3, 23.7; ESI-MS m/z calcd for $C_{37}H_{60}N_6O_{14}$ [M + H]⁺, 813.42458; found, 813.4; TOF-HRMS found, 813.42068. **Compound 14t**: 85%; [α]_D +7.3 (c 0.3, H₂O); ¹H NMR (400 MHz, D₂O) δ 6.95 (m, 1H), 6.15–6.05 (m, 3H), 5.67 (m, 1H), 5.24 (m, 1H), 5.13 (m, 1H), 4.41 (m, 1H), 4.14–2.8–4.07 (m, 5H), 3.90–3.55 (m, 12H), 3.46–3.11 (m, 8H), 2.34 (m, 1H), 1.79 (s, 18H), 1.67 (m, 1H); ¹³C NMR (125 MHz, D₂O) δ 181.7, 156.5, 149.2, 130.8, 129.1, 109.0, 107.5, 105.3, 96.3, 95.6, 85.6, 81.0, 79.1, 73.8, 73.5, 73.2, 70.6, 69.5, 69.2, 68.7, 68.0, 67.9, 67.6, 60.5, 60.3, 54.3, 51.2, 50.4, 49.3, 49.2, 40.6, 29.3, 23.5; ESI-MS m/z calcd for $C_{31}H_{54}N_6O_{15}$ [M + H]⁺, 751.37254; found, 751.6; TOF-HRMS found, 751.36768. **Compound 14u**: 90%; [α]_D +12.6 (c 0.8, H₂O); ¹H NMR (400 MHz, D₂O) δ 7.22–7.09 (m, 4H), 5.66 (m, 1H), 5.25 (m, 1H), 5.17 (m, 1H), 4.42 (m, 1H), 4.29–4.06 (m, 5H), 3.88–3.55 (m, 12H), 3.44–3.19 (m, 8H), 2.75–2.70 (m, 3H), 2.33 (m, 1H), 2.00–1.84 (m, 4H), 1.78 (s, 18H), 1.70 (m, 1H); ¹³C NMR (125 MHz, D₂O) δ 182.1, 139.1, 132.0, 130.7, 129.8, 129.1, 127.3, 110.3, 98.1, 97.5, 85.4, 82.2, 82.0, 76.0, 74.9, 74.2, 74.1, 72.7, 71.6, 71.4, 70.3, 69.5, 68.6, 67.3, 61.2, 61.1, 55.4, 52.2, 51.2, 50.2, 49.8, 41.3, 32.9, 28.8, 28.1, 24.2, 18.6; ESI-MS m/z calcd for $C_{35}H_{60}N_6O_{14}$ [M + H]⁺, 789.42458; found, 789.5; TOF-HRMS found, 789.42387. **Compound 14v**: 85%; [α]_D +4.9 (c 0.3, H₂O); ¹H NMR (400 MHz, D₂O) δ 5.68 (m, 1H), 5.26 (m, 1H), 5.17 (m, 1H), 4.42 (m, 1H), 4.28–4.07 (m, 5H), 3.88–3.59 (m, 12H), 3.47–3.19 (m, 8H), 2.70 (m, 1H), 2.34 (m, 1H), 2.1–0.8 (m, 39H); ¹³C NMR (125 MHz, D₂O) δ 182.2, 110.2, 98.5, 98.0, 85.2, 82.5, 82.0, 76.0, 75.3, 74.2, 74.0, 72.0, 71.8, 71.6, 70.4, 69.9, 68.8, 61.2, 55.5, 52.4, 52.2, 51.2, 50.4, 50.0, 41.4, 33.3, 31.1 (2C), 25.1, 24.6, 24.2, 24.1 (2C); ESI-MS m/z calcd for $C_{31}H_{60}N_6O_{14}$ [M + H]⁺, 741.41458; found, 741.5; TOF-HRMS found, 741.42466. **Compound 14w**: 80%; [α]_D +8.5 (c 0.6, H₂O); ¹H NMR (400 MHz, D₂O) δ 5.66 (m, 1H), 5.26 (m, 1H), 5.18 (m, 1H), 4.41 (m, 1H), 4.28–4.10 (m, 5H), 3.88–3.54 (m, 12H), 3.47–3.20 (m, 8H), 2.82 (m, 2H), 2.36–1.02 (m, 43H); ¹³C NMR (125 MHz, D₂O) δ 180.9, 108.5, 96.2, 95.1, 85.2, 80.9, 80.8, 77.6, 74.0, 73.7, 73.5, 73.0, 70.7, 69.8, 69.4, 68.0, 67.6, 65.7, 60.5, 54.1, 51.1, 49.0, 48.7, 47.2, 46.7, 42.4, 40.6, 35.8, 35.1, 32.6, 30.1, 29.7, 29.0, 28.5, 27.9, 23.2; ESI-MS m/z calcd for $C_{34}H_{66}N_6O_{14}$ [M + H]⁺, 781.45588; found, 781.5; TOF-HRMS found, 781.45282. **Compound 14x**: 80%; [α]_D +7.8 (c 0.5, H₂O); ¹H NMR (400 MHz, D₂O) δ 5.66 (m, 1H), 5.26 (m, 1H), 5.17 (m, 1H), 4.42 (m, 1H), 4.31–4.04 (m, 5H), 3.88–3.57 (m, 12H), 3.46–3.18 (m, 8H), 2.34 (m, 1H), 2.22 (m, 3H), 1.79 (s, 18H), 1.70–1.66 (m, 4H), 1.57 (m, 6H), 1.44 (m, 3H); ESI-MS m/z calcd for $C_{35}H_{66}N_6O_{15}$ [M + H]⁺, 809.45079; found, 809.4; TOF-HRMS found, 809.44818. **Compound 14y**: 80%; [α]_D +13.6 (c 0.8, H₂O); ¹H NMR (400 MHz, D₂O) δ 5.66 (m, 1H), 5.26 (m, 1H), 5.18 (m, 1H), 4.41 (m, 1H), 4.28–4.10 (m, 5H), 3.88–3.54 (m, 12H), 3.47–3.20 (m, 8H), 2.88 (m, 2H), 2.33 (m, 1H), 1.80 (s, 18H), 1.71 (m, 1H), 1.42 (m, 2H), 0.80 (m, 9H); ¹³C NMR (125 MHz, D₂O) δ 182.7, 109.6, 96.9, 94.3, 84.8, 81.3, 77.5, 75.2, 74.5, 73.7, 71.9, 70.8, 69.6, 69.2, 68.4, 67.8, 61.4, 60.3, 59.9, 54.8, 51.4, 50.5, 49.6, 47.5, 46.5, 40.2, 34.3 (3C), 31.6, 29.3, 26.1, 23.9; ESI-MS m/z calcd for $C_{31}H_{62}N_6O_{14}$ [M + H]⁺, 743.44023; found, 743.4; TOF-HRMS found, 743.43885. **Compound 14z**: 80%; [α]_D +7.4 (c 0.4, H₂O); ¹H NMR (400 MHz, D₂O) δ 5.66 (m, 1H), 5.26 (m, 1H), 5.18 (m, 1H), 4.41 (m, 1H), 4.28–4.10 (m, 5H), 3.88–3.54 (m, 12H), 3.47–3.20 (m, 8H), 2.31 (m, 1H), 2.01–0.65 (m, 66H); ESI-MS m/z calcd for $C_{52}H_{96}N_6O_{14}$ [M + H]⁺, 1029.70628; found, 1029.7; TOF-HRMS found, 1029.70511. **Compound 14aa**: 75%; [α]_D +8.4 (c 0.5, H₂O); ¹H NMR (400 MHz, D₂O) δ 8.61 (d, J = 3.5 Hz, 2H), 8.22 (d, J = 3.5 Hz, 2H), 7.77 (t, J = 7 Hz, 2H), 5.66 (m, 1H), 5.30 (m, 1H), 5.11 (m, 1H), 4.46 (m, 1H), 4.20–4.00 (m, 5H), 3.95–3.50 (m, 12H), 3.40–2.95 (m, 12H), 2.37 (m, 1H), 1.79 (s, 18H), 1.70 (m, 1H); ¹³C NMR (125 MHz, D₂O) δ 181.1, 165.4 (2C), 134.8 (2C), 129.7 (2C), 128.4 (2C), 126.4 (2C), 123.6 (2C), 110.7, 96.8, 96.1, 85.0, 82.3, 78.1, 76.1, 74.6, 73.2, 71.3, 70.8 (7C), 69.7, 68.8, 68.1, 67.6, 61.8, 61.1, 56.7, 54.6, 52.8, 51.7, 51.4, 50.8, 49.5, 41.6, 28.9, 23.4; ESI-MS m/z calcd for $C_{39}H_{61}N_7O_{16}$ [M + H]⁺, 882.40965;

found, 882.5; TOF-HRMS found, 882.40762. **Compound 14ab**: 80%; $[\alpha]_D +7.3$ (*c* 0.6, H₂O); ¹H NMR (400 MHz, D₂O) δ 5.76 (m, 1H), 5.46 (m, 1H), 5.26 (m, 1H), 4.62 (m, 1H), 4.41–4.04 (m, 5H), 3.90–3.50 (m, 14H), 3.45–3.20 (m, 6H), 2.9 (s, 6H), 2.33 (m, 1H), 1.88 (s, 18H), 1.70 (m, 1H); ¹³C NMR (125 MHz, D₂O) δ 182.0, 108.8, 96.7, 95.6, 85.8, 81.4, 81.2, 78.9, 74.3, 74.2, 73.9, 71.2, 69.9, 69.8, 68.5, 68.0, 64.9, 60.9, 59.9, 57.5, 54.7, 51.7, 50.9, 49.6, 43.6 (2C), 41.1, 30.2, 23.9; ESI-MS *m/z* calcd for C₂₇H₅₄N₆O₁₄ [M + H]⁺, 687.37763; found, 687.4; TOF-HRMS found, 687.37907. **Compound 14ac**: 90%; $[\alpha]_D +11.6$ (*c* 0.8, H₂O); ¹H NMR (400 MHz, D₂O) δ 7.31–7.23 (m, 10H), 5.74 (m, 1H), 5.36 (m, 1H), 5.27 (m, 1H), 4.29 (m, 1H), 4.21–4.07 (m, 5H), 3.90–3.14 (m, 24H), 2.78–2.69 (m, 4H), 2.35–2.23 (m, 3H), 1.89 (s, 18H), 1.61 (m, 1H); ESI-MS *m/z* calcd for C₄₂H₇₀N₆O₁₄ [M + H]⁺, 883.50283; found, 883.8; TOF-HRMS found, 883.49692. **Compound 14ad**: 80%; $[\alpha]_D +8.3$ (*c* 0.5, H₂O); ¹H NMR (400 MHz, D₂O) δ 5.69 (m, 1H), 5.33 (m, 1H), 5.13 (m, 1H), 4.50 (m, 1H), 4.20–4.00 (m, 5H), 3.90–3.52 (m, 12H), 3.41–3.02 (m, 8H), 2.72 (m, 4H), 2.33 (m, 1H), 1.84 (s, 18H), 1.62 (m, 1H), 1.53 (m, 4H), 1.29 (m, 20H) 0.88 (m, 6H); ¹³C NMR (125 MHz, D₂O) δ 182.1, 110.3, 98.3, 97.6, 85.4, 82.9, 82.2, 76.3, 75.8, 74.1, 72.1, 71.9, 71.6, 70.7, 69.9, 68.5, 67.8, 62.1, 61.7, 60.8, 56.5, 54.6, 51.5, 50.8 (2C), 50.5, 41.6, 33.7 (2C), 32.4 (2C), 30.8 (2C), 29.7 (2C), 29.1, 28.6 (2C), 24.2, 21.3 (2C), 16.4 (2C); ESI-MS *m/z* calcd for C₄₁H₈₂N₆O₁₄ [M + H]⁺, 883.59673; found, 883.9; TOF-HRMS found, 883.59434. **Compound 14ae**: 85%; $[\alpha]_D +14.5$ (*c* 0.7, H₂O); ¹H NMR (400 MHz, D₂O) δ 5.70 (m, 1H), 5.35 (m, 1H), 5.12 (m, 1H), 4.49 (m, 1H), 4.30–4.00 (m, 5H), 3.95–3.40 (m, 14H), 3.45–3.05 (m, 10H), 2.68 (m, 4H), 2.26 (m, 1H), 1.87 (s, 21H), 1.62 (m, 1H); ¹³C NMR (125 MHz, D₂O) δ 181.6, 108.9, 96.6, 95.9, 87.5, 81.6, 78.5, 74.6, 74.5, 73.7, 71.2, 70.0, 69.8, 68.5, 68.1, 68.0, 61.0, 60.6, 57.2, 54.7, 51.8, 51.1, 50.8, 50.2 (2C), 49.7, 43.6 (2C), 41.1, 31.1, 23.6; ESI-MS *m/z* calcd for C₂₉H₅₈N₇O₁₄ [M + H]⁺, 728.40417; found, 728.3; TOF-HRMS found, 728.40202.

Compound 15: To **11** (1.00 g, 0.654 mmol) in solution in pyridine (20 mL) was added Pb(OAc)₄ (725 mg, 1.635 mmol). After stirring overnight, oxalic acid (295 mg, 3.271 mmol) was added and the solvent was evaporated. The resulting yellow solid was taken up in EtOAc and the solids were filtered. The filtrate was washed with water and dried over Na₂SO₄, the solvent was removed under vacuum, and the resulting yellow oil was purified by silica gel chromatography (2% MeOH in CH₂Cl₂). The resulting yellow solid was dissolved in THF (20 mL) and Et₃N (5 mL) was added. After stirring for 36 h, the solvent was removed under vacuum and the oil was purified by silica gel chromatography (3% MeOH in CH₂Cl₂) to get **15** (220 mg, 30%) as a white solid. $[\alpha]_D +18.82$ (*c* 1.0, CHCl₃); *R*_f 0.6 (CHCl₃/EtOAc/MeOH (20:5:3)); ¹H NMR (300 MHz, CDCl₃) δ 7.60–7.10 (m, 20H), 6.30–3.00 (m, 30H), 2.27 (m, 1H), 1.33 (m, 1H), 0.85 (s, 9H), 0.03 (s, 6H); ESI-MS *m/z* calcd for C₅₇H₇₃N₃O₁₇Si [M + H]⁺, 1100.47875; found, 1100.6; TOF-HRMS found, 1100.47681.

Compound 16: A solution of **15** (200 mg, 0.182 mmol) in dry pyridine (10 mL) containing DMAP (2 mg) was treated with benzoyl chloride (0.21 mL, 1.812 mmol). The reaction mixture was stirred at room temperature for 16 h, water (1 mL) was added, and the solvent was removed under vacuum. The residue was dissolved in ethyl acetate, and the organic layer was washed with 0.5 M HCl, satd. NaHCO₃, and water, dried over Na₂SO₄, and concentrated under vacuum. The crude product was purified by silica gel flash chromatography (1:1 EtOAc/hexane) to yield the *O*-benzoyl-protected derivative **16** (240 mg, quant.); $[\alpha]_D +21.6$ (*c* 0.7, CHCl₃); *R*_f 0.5 (1:1 EtOAc/hexane); ¹H NMR (300 MHz, CDCl₃) δ 8.15–7.10 (m, 35H), 6.30–3.00 (m, 33H), 2.23 (m, 1H), 1.37 (m, 1H), 0.89 (s, 9H), 0.03 (s, 6H); ¹³C NMR (75 MHz, CDCl₃) δ 160.3, 158.6, 142.4, 139.4, 138.2, 137.5, 134.1, 131.6, 130.5, 129.4, 129.2, 129.1, 129.0, 128.9, 128.8, 128.7, 128.5, 128.3, 128.2, 128.1, 128.0, 126.7, 99.4, 84.5, 77.6, 71.8, 68.7, 67.9, 67.6, 67.2, 29.5; ESI-MS *m/z* calcd for C₇₈H₈₅N₃O₂₀Si [M + H]⁺, 1412.55439; found, 1412.9; TOF-HRMS found, 1412.55173.

Compounds 17a–c: The *O*-benzoyl-protected derivative **16** (250 mg, 0.177 mmol) in CH₂Cl₂ (15 mL) was cooled at –78 °C and

ozone was bubbled for 2 h, after which excess ozone was removed by bubbling argon. The mixture was treated with Me₂S (0.130 mL, 1.77 mmol) and warmed to room temperature and the solvent was removed under vacuum. The crude solid was purified by silica gel flash chromatography (2:3 EtOAc/hexane) to give the corresponding aldehyde (200 mg, 80%); *R*_f 0.25 (1:1 EtOAc/hexane); ESI-MS *m/z* calcd for C₇₇H₈₃N₃O₂₁Si [M + H]⁺, 1414.5; found, 1414.7. To a mixture of the above aldehyde (70 mg, 0.050 mmol) and appropriate amine (0.15 mmol) in dry MeOH (3 mL) was added acetic acid (0.1 mL), followed by NaBH₃CN (1.0 M in THF, 148 μ L, 0.148 mmol). A TLC indicated a complete disappearance of the aldehyde after 18 h. A freshly prepared solution of MeONa/MeOH was added dropwise until the pH reached approximately 10–10.5. When the reaction was complete, as indicated by a MS analysis, the solution was cooled down to –78 °C and dry ice was added until neutral pH. Solvent was removed under vacuum, and the residue was taken up in EtOAc, washed with water, and dried over Na₂SO₄. After removal of the solvent under vacuum, the solid was purified by silica gel flash chromatography to obtain the desired amine **17a–c**. **Compound 17a**: 64%; silica gel flash chromatography eluent, 3 to 5% MeOH/CH₂Cl₂; $[\alpha]_D +10.3$ (*c* 0.5, MeOH); *R*_f 0.2 (5% MeOH/CH₂Cl₂); ESI-MS *m/z* calcd for C₆₄H₈₂N₄O₁₇Si [M + H]⁺, 1207.6; found, 1208.2. **Compound 17b**: 77%; silica gel flash chromatography eluent, 3 to 5% MeOH/CH₂Cl₂; $[\alpha]_D +14.8$ (*c* 1.0, MeOH); *R*_f 0.15 (5% MeOH/CH₂Cl₂); ESI-MS *m/z* calcd for C₆₇H₈₇N₅O₁₉Si [M + H]⁺, 1294.6; found 1294.9. **Compound 17c**: 82%; silica gel flash chromatography eluent, 3 to 5% MeOH/CH₂Cl₂; $[\alpha]_D +11.7$ (*c* 0.9, MeOH); *R*_f 0.2 (5% MeOH/CH₂Cl₂); ESI-MS *m/z* calcd for C₆₄H₈₂N₄O₁₇Si [M + H]⁺, 1207.6; found, 1207.9.

Compounds 18a–c: The appropriate substrate **17a–c** was dissolved in 80% aqueous acetic acid (3 mL), and the solution was heated at 60 °C for 2–5 h or until a MS analysis showed total conversion of the starting material into the benzylidene as well as TBS-deprotected product. The solution was cooled down to room temperature, a catalytic amount of 20% palladium hydroxide on carbon was added, and the suspension was stirred at room temperature under an atmosphere of hydrogen (hydrogen balloon) until the conversion of the starting material into the product was completed, as indicated by MS analysis. The mixture was filtered through a layer of Celite on cotton, concentrated under vacuum, washed with CH₂Cl₂ twice, and lyophilized to afford compounds **18a–c** as fluffy white solids. **Compound 18a**: 75%; $[\alpha]_D +6.9$ (*c* 0.5, H₂O); ¹H NMR (400 MHz, D₂O) δ 5.67 (m, 1H), 5.34 (m, 1H), 4.35 (m, 1H), 4.22 (m, 1H), 3.99–3.12 (m, 16H), 2.81 (m, 2H), 2.21 (m, 1H), 1.82 (s, 12H), 1.53 (m, 1H); ¹³C NMR (125 MHz, D₂O) δ 182.6, 108.5, 96.4, 85.7, 83.3, 82.6, 73.9, 73.8, 73.5, 69.7, 69.6, 68.9, 66.6, 60.9, 60.6, 54.5, 50.8, 49.4, 39.8, 28.7, 23.5; ESI-MS *m/z* calcd for C₁₉H₃₈N₄O₁₁ [M + H]⁺, 499.26153; found, 499.4; TOF-HRMS found, 499.26104. **Compound 18b**: 85%; $[\alpha]_D +10.8$ (*c* 1.0, H₂O); ¹H NMR (400 MHz, D₂O) δ 5.66 (m, 1H), 5.34 (m, 1H), 4.35 (m, 1H), 4.24 (m, 1H), 3.99–2.97 (m, 20H), 2.49 (m, 2H), 2.21 (m, 1H), 2.03 (m, 2H), 1.82 (s, 15H), 1.54 (m, 1H); ¹³C NMR (125 MHz, D₂O) δ 182.3, 108.6, 96.8, 86.1, 83.7, 82.8, 80.3, 74.3, 74.1, 73.6, 70.0, 69.2, 66.0, 61.2, 61.0, 54.9, 51.1, 49.8, 48.2, 45.3, 37.3, 31.5, 24.5, 24.1; ESI-MS *m/z* calcd for C₂₂H₄₅N₅O₁₁ [M + H]⁺, 556.31938; found, 556.4; TOF-HRMS found, 556.31849. **Compound 18c**: 85%; $[\alpha]_D +7.8$ (*c* 0.9, H₂O); ¹H NMR (400 MHz, D₂O) δ 7.36–7.25 (m, 5H), 5.72 (m, 1H), 5.33 (m, 1H), 4.37 (m, 1H), 4.26 (m, 1H), 3.98–2.95 (m, 20H), 2.73 (m, 2H), 2.21 (m, 1H), 1.87 (s, 12H), 1.71 (m, 1H); ¹³C NMR (125 MHz, D₂O) δ 181.4, 132.3, 131.6, 129.5, 129.2, 128.7, 127.1, 126.8, 108.8, 96.2, 95.3, 85.3, 81.6, 78.0, 74.1, 73.1, 70.7, 69.6, 69.3, 68.0, 67.7, 60.7, 60.3, 54.2, 50.3, 49.2, 43.0, 40.7, 29.2, 23.5; ESI-MS *m/z* calcd for C₂₇H₄₆N₄O₁₁ [M + H]⁺, 602.3163; found, 603.32413; TOF-HRMS found, 603.32322.

4',6'-O-Benzylidene-2''-O-cinnamyl-5''-O-*t*-butyldimethylsilylpenta-*N*-benzyloxycarbonyl Paromomycin (19). Procedure A: The alcohol **10** (6.00 g, 4.367 mmol) dried by two codistillations with toluene was dissolved in CH₂Cl₂ (400 mL) and 2,4,6-collidine (1.15 mL, 8.735 mmol) followed by TBDMSOTf (0.50 mL, 2.184

mmol) were added at 0 °C. After 18 h, 0.6 equiv of TBDMSOTf was added, and 6 h later, some of the CH₂Cl₂ was evaporated to a smaller volume for washing with HCl (0.5 M) twice and H₂O. Drying with Na₂SO₄ and purification by silica gel chromatography (2% MeOH/CH₂Cl₂) gave the O^{5''}-TBS monoprotected compound (4.861 g, 75%): [α]_D+41.8 (c 0.9, CHCl₃); R_f 0.6 (CHCl₃/EtOAc/MeOH (20:5:3)); ¹H NMR (300 MHz, CDCl₃) δ 7.60–7.10 (m, 30H), 5.60–3.00 (m, 41H), 2.20 (m, 1H), 1.30 (m, 1H), 0.83 (s, 9H), 0.01 (s, 6H); ESI-MS *m/z* calcd for C₇₆H₉₃N₅O₂₄Si [M + H]⁺, 1487.60580; found, 1488.9; TOF-HRMS found, 1488.60258. This O^{5''}-TBS monoprotected compound (200 mg, 0.134 mmol) was dissolved in dry THF (10 mL). A catalytic amount of Bu₄Ni and cinnamyl bromide (66 mg, 0.269 mmol) were added followed by the dropwise addition of 0.5 M KHMDs solution in toluene (0.350 mL, 0.175 mmol). The mixture was stirred overnight at room temperature, then 0.3 equiv of KHMDs was added, and 6 h later, the reaction mixture was quenched with an aqueous solution of satd. NH₄Cl (2 mL) and water. THF was evaporated and the aqueous layer was extracted with EtOAc. The organic layer was washed with a sodium thiosulfate solution and brine and dried over Na₂SO₄. The solvent was evaporated to dryness to afford a crude solid, which was purified by silica gel flash chromatography (1 to 2% MeOH in CH₂Cl₂), providing the corresponding cinnamyl ether **19** (152 mg, 70%): [α]_D+16.4 (c 1.0, CHCl₃); R_f 0.7 (CHCl₃/EtOAc/MeOH (20:5:3)); ¹H NMR (300 MHz, CDCl₃) δ 7.65–7.12 (m, 35H), 6.54–3.05 (m, 45H), 2.24 (m, 1H), 1.36 (m, 1H), 0.84 (s, 9H), 0.01 (s, 6H); ESI-MS *m/z* calcd for C₈₅H₁₀₁N₅O₂₄Si [M + H]⁺, 1604.66840; found, 1605.1; TOF-HRMS found, 1604.67026.

Procedure B: To **11** (200 mg, 0.131 mmol) in solution in CH₂-Cl₂ (0.01M) was added the Grubbs second generation catalyst (11 mg, 0.013 mmol), and after 16 h, the solution was heated to reflux for an additional 24 h. The solvent was removed under vacuum and the resulting brown solid was purified by silica gel chromatography (3% MeOH in CH₂Cl₂) to give the above described **19** (160 mg, 75%) as a white solid.

2''-O-(3-Phenylpropyl)-paromomycin (20). Compound **19** (100 mg, 0.062 mmol) was dissolved in 80% aqueous acetic acid (3 mL), and the solution was heated at 60 °C until a MS analysis showed total conversion of the starting material into the benzylidene as well as TBS-deprotected product (5 h). The solution was cooled down to room temperature, a catalytic amount of 20% palladium hydroxide on carbon was added, and the suspension was stirred at room temperature under an atmosphere of hydrogen (hydrogen balloon) until the conversion of the starting material into the product was completed, as indicated by MS analysis. The mixture was filtered through a layer of Celite on cotton, concentrated under vacuum, washed with CH₂Cl₂ twice, and lyophilized to afford **20** as a fluffy white solid (32 mg, 70%): [α]_D+10.5 (c 0.6, H₂O); ¹H NMR (400 MHz, D₂O) δ 7.28–7.19 (m, 5H), 5.67 (m, 1H), 5.32 (m, 1H), 5.13 (m, 1H), 4.47 (m, 1H), 4.14–4.11 (m, 5H), 3.86–3.51 (m, 12H), 3.40–3.19 (m, 6H), 2.61–2.36 (m, 4H), 2.31 (m, 1H), 1.84 (s, 15H), 1.71 (m, 1H); ¹³C NMR (125 MHz, D₂O) δ 181.9, 142.3, 129.1 (2C), 128.9 (2C), 126.5, 108.7, 96.2, 95.5, 85.4, 81.8, 80.9, 78.0, 74.3, 74.1, 73.1, 71.8, 70.7, 69.9, 69.6, 69.3, 68.0, 67.9, 67.7, 60.4, 54.2, 51.3, 50.3, 49.2, 40.7, 31.7, 30.7, 23.8; ESI-MS *m/z* calcd for C₃₂H₅₅N₅O₁₄ [M + H]⁺, 734.38238; found, 734.5; TOF-HRMS found, 734.38213.

Compound 21: To cinnamyl triphenylphosphonium bromide (31 mg, 0.081 mmol) in solution in THF (1 mL) was added KHMDs (0.5 M in toluene, 0.17 mL, 0.085 mmol), and the resulting orange solution was added to a solution of **12** (75 mg, 0.041 mmol) in THF (3 mL) at –40 °C. After 1 h, the solution was warmed to 0 °C for 2 h. NH₄Cl was added, the solvent was removed under vacuum, and the resulting yellow solid was taken up in EtOAc, washed with water, and dried over Na₂SO₄. The solvent was removed under vacuum to give the olefin that was used directly in the next step. To this olefin dissolved in MeOH was added a freshly prepared solution of MeONa/MeOH until the pH reached approximately 10–10.5. When the reaction was finished as indicated by a MS analysis, the solution was cooled down to –78 °C and dry ice was added until neutral pH. Solvent was removed under

vacuum, and the residue was taken up in EtOAc, washed with water, and dried over Na₂SO₄. After removal of the solvent under vacuum, the solid was purified by silica gel flash chromatography to obtain **21** (25 mg, 82%): [α]_D+21.8 (c 0.9, CHCl₃); R_f 0.7 (CHCl₃/EtOAc/MeOH (20:5:3)); ¹H NMR (300 MHz, CDCl₃) δ 7.60–7.10 (m, 35H), 6.57–3.00 (m, 47H), 2.25 (m, 1H), 1.41 (m, 1H), 0.91 (s, 9H), 0.02 (s, 6H); ESI-MS *m/z* calcd for C₈₇H₁₀₃N₅O₂₄Si [M + Na]⁺, 1652.66600; found, 1653.9; TOF-HRMS found, 1652.66981.

2''-O-(5-Phenylpentyl)-paromomycin (22). The ether **21** was dissolved in 80% aqueous acetic acid (3 mL), and the solution was heated at 60 °C until a MS analysis showed total conversion of the starting material into the benzylidene as well as TBS-deprotected product (5 h). The solution was cooled down to room temperature, a catalytic amount of 20% palladium hydroxide on carbon was added, and the suspension was stirred at room temperature under an atmosphere of hydrogen (hydrogen balloon) until the conversion of the starting material into the product was completed, as indicated by MS analysis. The mixture was filtered through a layer of Celite on cotton, concentrated under vacuum, washed with CH₂Cl₂ twice, and lyophilized to afford **22** as a fluffy white solid (11 mg, 70%): [α]_D+10.5 (c 0.6, H₂O); ¹H NMR (400 MHz, D₂O) δ 7.36–7.26 (m, 5H), 5.69 (m, 1H), 5.43 (m, 1H), 5.12 (m, 1H), 4.39 (m, 1H), 4.18–4.12 (m, 5H), 3.93–3.04 (m, 18H), 2.63 (m, 2H), 2.22 (m, 1H), 1.90 (s, 15H), 1.71 (m, 1H), 1.64 (m, 4H), 1.35 (m, 2H); ¹³C NMR (125 MHz, D₂O) δ 182.6, 141.0, 129.7 (2C), 129.1 (2C), 125.9, 107.6, 97.7, 96.3, 84.9, 82.3, 81.2, 78.4, 74.5, 74.3, 72.1, 71.2, 70.4, 69.8, 68.5, 68.0, 62.7, 61.9, 60.1, 54.1, 50.8, 49.7, 49.2, 40.6, 37.3, 33.4, 32.5, 28.7, 26.4, 23.9; ESI-MS *m/z* calcd for C₃₄H₅₉N₅O₁₄ [M + H]⁺, 762.41368; found, 762.4; TOF-HRMS found, 762.41423.

Compound 23. Procedure A: A solution of **12** (100 mg, 0.055 mmol) in THF (5 mL) was cooled down to –40 °C and PhMgBr (1 M in THF, 81 μL, 0.081 mmol) was slowly added. After 1 h, a few drops of satd. NH₄Cl was added, the solvent was evaporated, the resulting solid was taken up in AcOEt, washed with water, and dried over Na₂SO₄, and the solvent was evaporated. **Procedure B:** Alternatively, Ph₂Zn (24 mg, 0.109 mmol) was added to a solution of **12** (100 mg, 0.055 mmol) in THF (5 mL) at room temperature and NH₄Cl was added after 30 min. This later procedure was used without affecting any benzoate ester protecting group.

To the combined alcohol dissolved in MeOH was added a freshly prepared solution of MeONa/MeOH until the pH reached approximately 10–10.5. When the reaction was finished, as indicated by a MS analysis, the solution was cooled down to –78 °C and dry ice was added until neutral pH. Solvent was removed under vacuum, and the residue was taken up in EtOAc, washed with water, and dried over Na₂SO₄. After removal of the solvent under vacuum, the resulting solid was purified by silica gel flash chromatography (2% MeOH in CH₂Cl₂) to obtain **23** (108 mg, 65%): [α]_D+16.2 (c 0.7, CHCl₃); R_f 0.6 (CHCl₃/EtOAc/MeOH (20:5:3)); ¹H NMR (300 MHz, CDCl₃) δ 7.60–7.10 (m, 35H), 5.65–3.12 (m, 45H), 2.21 (m, 1H), 1.35 (m, 1H), 0.91 (s, 9H), 0.03 (s, 6H); ESI-MS *m/z* calcd for C₈₄H₁₀₁N₅O₂₅Si [M + Na]⁺, 1630.64526; found, 1632.2; TOF-HRMS found, 1630.64331.

2''-O-(2-Phenylethyl)-paromomycin (25) and Hydroxyl Analogue (24). Compound **23** (150 mg, 0.093 mmol) was dissolved in 80% aqueous acetic acid (3 mL), and the solution was heated at 60 °C until a MS analysis showed total conversion of the starting material into the benzylidene as well as TBS-deprotected product (5 h). The solvent was removed and replaced by 3 mL of MeOH/water (1:1), a catalytic amount of 20% palladium hydroxide on carbon was added, and the suspension was stirred at room temperature under an atmosphere of hydrogen (hydrogen balloon) until the conversion of the starting material into the product was completed, as indicated by MS analysis. After 6 h, half of the mixture (1.5 mL) was filtered through a layer of Celite on cotton, concentrated under vacuum, washed with CH₂Cl₂ twice, and lyophilized to afford a fluffy white solid **24** (21 mg, 70%). To the remaining half AcOH (1.5 mL) was added and the hydrogenation was pursued for an additional 18 h to provide **25** (24 mg, 80%).

Compounds 24 and 25. Compound 24: [α]_D+9.2 (c 0.5, H₂O);

References

- (1) Walsh, C. *Antibiotics: Actions, Origins, Resistance*; ASM Press: Washington, DC, 2003.
- (2) Waskman, S. A.; Bugie, E.; Schatz, A. Isolation of antibiotic substances from soil microorganisms, with special reference to streptothricin and streptomycin. *Proc. Staff Meet. Mayo Clin.* **1944**, *19*, 537–548.
- (3) Vakulenko, S. B.; Mobashery, S. Versatility of aminoglycosides and prospects for their future. *Clin. Microbiol. Rev.* **2003**, *16*, 430–450.
- (4) (a) Mingeot-Leclercq, M. P.; Tulkens, P. M. Aminoglycosides: Nephrotoxicity. *Antimicrob. Agents Chemother.* **1999**, *43*, 1003–1012. (b) Mingeot-Leclercq, M. P.; Glupczynski, Y.; Tulkens, P. M. Aminoglycosides: Activity and resistance. *Antimicrob. Agent. Chemother.* **1999**, *43*, 727–737.
- (5) (a) Magnet, S.; Blanchard, J. S. Molecular Insights into Aminoglycoside Action and Resistance. *Chem. Rev.* **2005**, *105*, 477–497. (b) Fong, D. H.; Berghuis, A. M. Substrate promiscuity of an aminoglycoside antibiotic resistance enzyme via target mimicry. *EMBO J.* **2002**, *21*, 2323–2331. (c) Smith, C. A.; Baker, E. N. Aminoglycoside antibiotic resistance by enzymatic deactivation. *Curr. Drug Targets Infect. Disord.* **2002**, *2*, 143–160. (d) Davies, J. Inactivation of antibiotics and the dissemination of resistance genes. *Science* **1994**, *264*, 375–382. (e) Shaw, K. J.; Rather, P. N.; Hare, R. S.; Miller, G. H. Molecular genetics of aminoglycoside resistance genes and familial relationships of the aminoglycoside-modifying enzymes. *Microbiol. Rev.* **1993**, *57*, 138–163.
- (6) Parsek, M. R.; Singh, P. K. Bacterial biofilms: An emerging link to disease pathogenesis. *Annu. Rev. Microbiol.* **2003**, *57*, 677–701.
- (7) (a) Parke, Davis and Company, Belgian Patent 547976, 1956. (b) Haskell, T. H.; Hanessian, S. The configuration of paromose. *J. Org. Chem.* **1963**, *28*, 2598–2604.
- (8) Varandani, R. S.; Sharma, S. N. Release rate of neomycin sulfate from ointment bases containing hydrocortisone acetate. *East. Pharm.* **1982**, *25*, 113–115.
- (9) Wright, G. D. Aminoglycoside-modifying enzymes. *Curr. Opin. Microbiol.* **1999**, *2*, 499–503.
- (10) Balwit, J. M.; van Langevelde, P.; Vann, J. M.; Proctor, R. A. Gentamicin-resistant menadione and hemin auxotrophic *Staphylococcus aureus* persist within cultured endothelial cells. *J. Infect. Dis.* **1994**, *170*, 1033–1037.
- (11) Putman, M.; van Veen, H. W.; Konings, W. N. Molecular properties of bacterial multidrug transporters. *Microbiol. Mol. Biol. Rev.* **2000**, *64*, 672–693.
- (12) (a) Doi, Y.; Yokoyama, K.; Yamane, K.; Wachino, J.; Shibata, N.; Yagi, T.; Shibayama, K.; Kato, H.; Arakawa, Y. Plasmid-mediated 16S rRNA methylase in *Serratia marcescens* conferring high-level resistance to aminoglycosides. *Antimicrob. Agents Chemother.* **2004**, *48*, 491–496. (b) Galimand, M.; Courvalin, P.; Lambert, T. Plasmid-mediated high-level resistance to aminoglycosides in Enterobacteriaceae due to 16S rRNA methylation. *Antimicrob. Agents Chemother.* **2003**, *47*, 2565–2571. (c) Cundliffe, E. How antibiotic-producing organisms avoid suicide. *Annu. Rev. Microbiol.* **1989**, *43*, 207–233.
- (13) (a) Noller, H. F. RNA structure: Reading the ribosome. *Science* **2005**, *309*, 1508–1514. (b) Woodcock, J.; Moazed, D.; Cannon, M.; Davies, J.; Noller, H. F. Interaction of antibiotics with A- and P-site-specific bases in 16S ribosomal RNA. *EMBO J.* **1991**, *10*, 3099–3103. (c) Gale, E. F.; Cundliffe, E.; Reynolds, P. E.; Richmond, M. H.; Waring, M. J. *The Molecular Basis of Antibiotic Action*; Wiley: London, 1981. (d) Moazed, D.; Noller, H. F. Interaction of antibiotics with functional sites in 16S ribosomal RNA. *Nature* **1987**, *327*, 389–394.
- (14) Wimberly, B. T.; Brodersen, D. E.; Clemons, J. W. M.; Morgan-Warren, R. J.; Caster, A. P.; Vonrhein, C.; Hartsek, T.; Ramakrishnan, V. Structure of the 30S ribosomal subunit. *Nature* **2000**, *407*, 327–339.
- (15) (a) Carter, A. P.; Clemons, W. M.; Bordersen, D. E.; Morgan-Warren, R. J.; Wimberly, B. T.; Ramakrishnan, V. Functional insights from the structure of the 30S ribosomal subunit and its interactions with antibiotics. *Nature* **2000**, *407*, 340–348. (b) Ogle, J. M.; Brodersen, D. E.; Clemons, W. M., Jr.; Tarry, M. J.; Carter, A. P.; Ramakrishnan, V. Recognition of cognate transfer RNA by the 30S ribosomal subunit. *Science* **2001**, *292*, 897–902.
- (16) (a) Vicens, Q.; Westhof, E. Crystal structure of paromomycin docked into the eubacterial ribosomal decoding A site. *Structure* **2001**, *9*, 647–658. (b) Vicens, Q.; Westhof, E. Crystal structure of a complex between the aminoglycoside tobramycin and an oligonucleotide containing the ribosomal decoding A site. *Chem. Biol.* **2002**, *9*, 747–755. (c) Vicens, Q.; Westhof, E. Crystal structure of geneticin bound to a bacterial 16S ribosomal RNA A site oligonucleotide. *J. Mol. Biol.* **2003**, *326*, 1175–1188. (d) Pfister, P.; Hobbie, S.; Vicens, Q.; Böttger, E. C.; Westhof, E. The molecular basis for A-site mutations conferring aminoglycoside resistance: Relationship between ribosomal susceptibility and X-ray crystal structures. *ChemBioChem* **2003**, *4*, 1078–1088. (e) François, B.; Russell, R. J.; Murray, J. B.; Aboul-ela, F.; Masquida, B.; Vicens, Q.; Westhof, E. Crystal structures of complexes between aminoglycosides and decoding A site oligonucleotides: Role of the number of rings and positive charges in the specific binding leading to miscoding. *Nucleic Acids Res.* **2005**, *33*, 5677–5690. (f) Kondo, J.; François, B.; Russell, R. J.; Murray, J. B.; Westhof, E. Crystal structure of the bacterial ribosomal decoding site complexed with amikacin containing the γ -amino- α -hydroxybutyryl (haba) group. *Biochimie* **2006**, *88*, 1027–1031.
- (17) See, for example: Recht, M. I.; Fourmy, D.; Blanchard, K. D.; Dahlquist, D.; Puglisi, J. D. RNA sequence determinants for aminoglycoside binding to an A-site rRNA model oligonucleotide. *J. Mol. Biol.* **1999**, *262*, 421–436.
- (18) Fourmy, D.; Recht, M. I.; Blanchard, S. C.; Puglisi, J. D. Structure of the A site of *Escherichia coli* 16S ribosomal RNA complexed with an aminoglycoside antibiotic. *Science* **1996**, *274*, 1367–1371.
- (19) (a) Hofstadler, S. A.; Griffey, R. H. Mass spectrometry as a drug discovery platform against RNA targets. *Curr. Opin. Drug Discovery Dev.* **2000**, *3*, 423–431. (b) Griffey, R. H.; Hofstadler, S. A.; Sannes-Lowery, K. A.; Ecker, D. J.; Crooke, S. T. Determinants of aminoglycoside-binding specificity for rRNA by using mass spectrometry. *Proc. Natl. Acad. Sci. U.S.A.* **1999**, *96*, 10129–10133. (c) Griffey, R. H.; Greig, M. J.; An, H.; Sasmor, H.; Manalili, S. Targeted site-specific gas-phase cleavage of oligoribonucleotides. Application in mass spectrometry-based identification of ligand binding sites. *J. Am. Chem. Soc.* **1999**, *121*, 474–475.
- (20) (a) Fourmy, D.; Yoshizawa, S.; Puglisi, J. D. Paromomycin binding induces a local conformational change in the A-site of 16S rRNA. *J. Mol. Biol.* **1998**, *277*, 333–345. (b) Fourmy, D.; Recht, M. I.; Puglisi, J. D. Binding of neomycin-class aminoglycoside antibiotics to the A-site of 16S rRNA. *J. Mol. Biol.* **1998**, *277*, 347–362. (c) Lynch, S. R.; Gonzalez, R. L., Jr.; Puglisi, J. D. Comparison of X-ray crystal structure of the 30S subunit–antibiotic complex with NMR structure of decoding site oligonucleotide–paromomycin complex. *Structure* **2003**, *11*, 43–53.
- (21) (a) Moitessier, N.; Hanessian, S.; Westhof, E. Docking of aminoglycosides to hydrated and flexible RNA. *J. Med. Chem.* **2006**, *43*, 1023–1033. (b) Hermann, T.; Westhof, E. Docking of cationic antibiotics to negatively charged pockets in RNA folds. *J. Med. Chem.* **1999**, *42*, 1250–1261. (c) Leclerc, F.; Cedergren, R. Modeling RNA–ligand interactions: The Rev-binding element RNA–aminoglycoside complex. *J. Med. Chem.* **1998**, *41*, 175–182.
- (22) (a) Rai, R.; Chen, H.-N.; Czyryca, P. G.; Li, J.; Chang, C.-W. T. Design and synthesis of pyrankacin: A pyranmycin class of broad-spectrum aminoglycoside antibiotic. *Org. Lett.* **2006**, *8*, 887–889. (b) Hainrichson, M.; Pokrovskaya, V.; Shallom-Shezifi, D.; Fridman, M.; Belakhov, V.; Shachar, D.; Yaron, S.; Baasov, T. Branched aminoglycosides: Biochemical studies and antibacterial activity of neomycin B derivatives. *Bioorg. Med. Chem.* **2005**, *13*, 5797–5807. (c) Ding, Y.; Hofstadler, S. A.; Swayze, E. E.; Risen, L.; Griffey, R. H. Design and synthesis of paromomycin-related heterocycle-substituted aminoglycoside mimetics based on a mass spectrometry RNA-binding assay. *Angew. Chem., Int. Ed.* **2003**, *42*, 3409–3412. (d) Haddad, J.; Kotra, L. P.; Llano-Sotelo, B.; Kim, C.; Azucena, E. F., Jr.; Liu, M.; Vakulenko, S. B.; Chow, C. S.; Mobashery, S. Design of novel antibiotics that bind to the ribosomal acyltransfer site. *J. Am. Chem. Soc.* **2002**, *124*, 3229–3237. (e) Rosenbohm, C.; Vanden Berghe, D.; Vlietinck, A.; Wengel, J. Parallel synthesis of a small library of novel amino glycoside analogs based on 2-amino-2-deoxy-D-glucose and D-ribose scaffolds. *Tetrahedron* **2001**, *57*, 6277–6287. (f) Sucheck, S. J.; Greenberg, W. A.; Tolbert, J. J.; Wong, C.-H. Design of small molecules that recognize RNA: Development of aminoglycosides as potential antitumor agents that target oncogenic RNA sequences. *Angew. Chem., Int. Ed.* **2000**, *39*, 1080–1084. (g) Michael, K.; Wang, H.; Tor, Y. Enhanced RNA binding of dimerized amino glycosides. *Bioorg. Med. Chem.* **1999**, *7*, 1361–1371. (h) Nunns, C. L.; Spence, L. A.; Slater, M. J.; Berrisford, D. J. Synthesis of neamine libraries for RNA recognition using solution phase chemistry. *Tetrahedron Lett.* **1999**, *40*, 9341–9345. (i) Roestamadji, J.; Mobashery, S. The use of neamine as a molecular template: inactivation of bacterial antibiotic resistance enzyme aminoglycoside 3'-phosphotransferase type IIa. *Bioorg. Med. Chem. Lett.* **1998**, *8*, 3483–3488 and references cited therein.
- (23) Russell, R. J. M.; Murray, J. B.; Lentzen, G.; Haddad, J.; Mobashery, S. The complex of a designer antibiotic with a model aminoacyl site of the 30S ribosomal subunit revealed by X-ray crystallography. *J. Am. Chem. Soc.* **2003**, *125*, 3410–3411.
- (24) Vicens, Q.; Westhof, E. As a drug target: The case of aminoglycosides. *ChemBioChem* **2003**, *4*, 1018–1023.

- (25) François, B.; Szychowski, J.; Adhikari, S. S.; Pachamuthu, K.; Swayze, E. E.; Griffey, R. H.; Migawa, M. T.; Westhof, E.; Hanessian, S. Antibacterial aminoglycosides with a modified mode of binding to the ribosomal-RNA decoding site. *Angew. Chem., Int. Ed.* **2004**, *43*, 6735–6738.
- (26) Hanessian, S.; Takamoto, T.; Massé, R.; Patil, G. Aminoglycoside antibiotics: Chemical conversion of neomycin B, paromomycin, and lividomycin B into bioactive pseudosaccharides. *Can. J. Chem.* **1978**, *56*, 1482–1491.
- (27) Scholl, M.; Ding, S.; Lee, C. W.; Grubbs, R. H. Synthesis and activity of a new generation of ruthenium-based olefin metathesis catalysts coordinated with 1,3-dimesityl-4,5-dihydroimidazol-2-ylidene ligands. *Org. Lett.* **1999**, *1*, 953–956.
- (28) Carter, C. W. J. *Methods in Enzymology*; Academic Press: New York, 1996; p 276.
- (29) Navaza, J. *AMoRe*: an automated package for molecular replacement. *Acta Crystallogr., Sect. A* **1994**, *50*, 157–163.
- (30) Brünger, A. T.; Adams, P. D.; Clore, G. M.; DeLano, W. L.; Gros, P.; Grosse-Kunstleve, R. W.; Jiang, J.-S.; Kuszewski, J.; Nilges, M.; Pannu, N. S.; Read, R. J.; Rice, L. M.; Simonson, T.; Warren, G. L. Crystallography and NMR system: A new software suite for macromolecular structure determination. *Acta Crystallogr., Sect. D* **1998**, *54*, 905–921.
- (31) Kleywegt, G. J.; Jones, T. A. Databases in protein crystallography. *Acta Crystallogr., Sect. D* **1998**, *54*, 1119–1131.

JM061200+